Journal of Medicinal Chemistry

Article

Identification of GDC-0810 (ARN-810), an orally bioavailable Selective Estrogen Receptor Degrader (SERD) that demonstrates robust activity in tamoxifen-resistant breast cancer xenografts

Andiliy Lai, Mehmet Kahraman, Steven Govek, Johnny Nagasawa, Celine Bonnefous, Jackie Julien, Karensa Douglas, John Sensintaffar, Nhin Lu, Kyoung-jin Lee, Anna Aparicio, Josh Kaufman, Jing Qian, Gang Shao, Rene Prudente, Michael J Moon, James D Joseph, Beatrice Darimont, Daniel Brigham, Kate Grillot, Richard Heyman, Peter J Rix, Jeffrey H Hager, and Nicholas D Smith

J. Med. Chem., **Just Accepted Manuscript** • DOI: 10.1021/acs.jmedchem.5b00054 • Publication Date (Web): 16 Apr 2015

Journal of Medicinal Chemistry is published by the American Chemical Society. 1155 Sixteenth Street N.W., Washington, DC 20036

Identification of GDC-0810 (ARN-810), an orally bioavailable Selective Estrogen Receptor Degrader (SERD) that demonstrates robust activity in tamoxifen-resistant breast cancer xenografts

Andiliy Lai,[a] Mehmet Kahraman,[a] Steven Govek,[a] Johnny Nagasawa,[a] Celine Bonnefous,[a] Jackie Julien,[a] Karensa Douglas,[a] John Sensintaffar,[b] Nhin Lu,[b] Kyoung-jin Lee,[c] Anna Aparicio,[c] Josh Kaufman,[c] Jing Qian,[b] Gang Shao,[b] Rene Prudente,[b] Michael J. Moon,[b] James D. Joseph,[b] Beatrice Darimont,[b] Daniel Brigham,[b] Kate Grillot,[b] Richard Heyman,[b] Peter J. Rix,[c] Jeffrey H. Hager,[b] Nicholas D. Smith[a]*

Seragon Pharmaceuticals, 12780 El Camino Real, Suite 302, San Diego, California 92130.

[a] Department of Chemistry, [b] Department of Biology, [c] Department of Drug Safety and Disposition

ABSTRACT

Approximately eighty percent of breast cancers are estrogen receptor alpha (ER-α) positive, and although women typically initially respond well to anti-hormonal therapies such as tamoxifen and aromatase inhibitors, resistance often emerges. Although a variety of resistance mechanism

may be at play in this state, there is evidence that in many cases the ER still plays a central role, including mutations in the ER leading to constitutively active receptor. Fulvestrant is a steroid-based, selective estrogen receptor degrader (SERD) that both antagonizes and degrades ER-α, and is active in patients who have progressed on anti-hormonal agents. However fulvestrant suffers from poor pharmaceutical properties and must be administered by intra-muscular injections that limit the total amount of drug that can be administered, and hence lead to the potential for incomplete receptor blockade. We describe the identification and characterization of a series of small-molecule, orally bioavailable SERDs which are potent antagonists and degraders of ER-α, and in which the ER-α degrading properties were prospectively optimized. The lead compound **11l** (GDC-0810 or ARN-810) demonstrates robust activity in models of tamoxifen-sensitive and tamoxifen-resistant breast cancer, and is currently in clinical trials in women with locally advanced or metastatic estrogen receptor-positive breast cancer.

KEYWORDS: Estrogen receptor, estrogen receptor degrader, SERD, antagonist, tamoxifen-resistant, breast cancer, indazole, GDC-0810, ARN-810.

INTRODUCTION

The estrogen receptors ER-α and ER-β are members of the nuclear hormone receptor superfamily, and are ligand-regulated transcription factors that mediate the activity of estrogens in a number of important physiological processes, including reproduction, cardiovascular maintenance and bone density/remodeling.[1] ER-α has been an important target in the pharmaceutical industry for many years, with ER antagonists such as tamoxifen (**1**), and aromatase inhibitors (that block the production of estrogen) such as anastrozole being a mainstay in the treatment of ER-positive breast cancer.[2] Tamoxifen (**1**) and its active metabolite 4-

hydroxytamoxifen (**2**) (Figure 1) are selective estrogen receptor modulators (SERMs), in that they can behave as agonists or antagonists depending on the tissue context.[1] Unfortunately, despite many women with breast cancer initially responding well to tamoxifen, resistance often emerges. Although a variety of resistance mechanism may be at play in this state,[3] there is evidence that in many cases ER still plays a central role, and that tumor cells still utilize pro-growth signaling pathways down-stream of ER.[4] Recently, there has been increasing clinical evidence following treatment with aromatase inhibitors, of the involvement of mutations in the ligand-binding domain of ER-α rendering it transcriptionally active in the absence of ligand, leading to resistance to anti-hormonal therapy.[5] Based on this observation it might be expected that a next-generation ER-α ligand that both antagonizes and degrades (i.e. removes) the ER-α would be of benefit to patients that have progressed on anti-hormonal therapy such as tamoxifen or aromatase inhibitors.

Figure 1: Estrogen receptor ligands

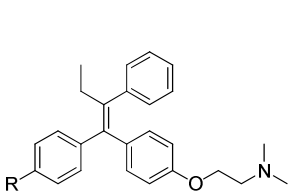

1: R = H: Tamoxifen
2: R = OH: 4-Hydroxytamoxifen

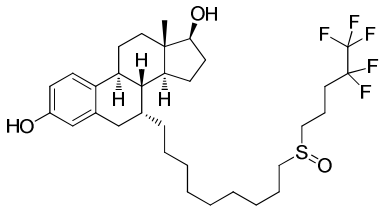

3: Fulvestrant

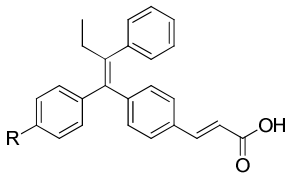

4: R = H: GW-5638
5: R = OH: GW-7604

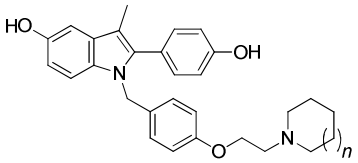

6: Pipendoxifene (*n* = 1)
7: Bazedoxifene (*n* = 2)

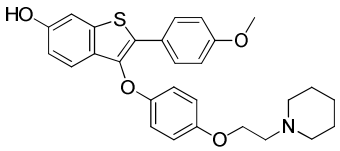

8: Arzoxifene

Fulvestrant (**3**) is a steroid-based estrogen receptor antagonist originally selected for development due its lack of agonism across all tissue types tested; however, it was retrospectively found to also be a selective estrogen receptor degrader (SERD) as well as antagonist.[6] Fulvestrant is approved for the treatment of ER-positive, metastatic breast cancer in postmenopausal women whose disease has progressed following treatment with endocrine therapy (i.e. tamoxifen or an aromatase inhibitor). However, fulvestrant is limited by poor pharmaceutical properties and is being administered by intra-muscular injections (500 mg total dose in 2 x 5mL injections), that limits the total amount of drug that may be administered and hence circulating levels. Even at the recently approved higher dose of 500 mg, FES-PET imaging data supports the notion that the limitations of fulvestrant intra-muscular dosing leads to incomplete estrogen receptor engagement in the clinic.[7] GW-5638 (**4**) is a non-steroidal ER antagonist originally selected for development for its lack of undesired uterotrophic activity in tamoxifen treated animals and patients, but like fulvestrant, was also retrospectively determined

to be a SERD.[8] Like tamoxifen, GW-5638 may be considered a prodrug as it is metabolized to produce the active metabolite GW-7604 (**5**) *in-vivo*. Importantly, tamoxifen-resistant breast cancer cell lines were not cross-resistant to GW-5638 treatment, and the compound was ultimately progressed to a Phase 1 clinical trial, although development was discontinued for unknown reasons. Thus the activity of fulvestrant in relapsed patients in the clinic, and GW-5638 in models of tamoxifen-resistance, support the notion that ER still plays a critical role in tamoxifen-resistant breast cancer. We therefore set out to identify non-steroidal SERDs where the ER-α degradation efficacy of the compounds was optimized prospectively, and were orally bioavailable allowing rapid achievement of robust, therapeutic levels of exposure.

CHEMISTRY

The compounds presented in this manuscript were prepared as outlined in Schemes 1 to 6. The synthetic strategy involved preparation of an appropriately substituted alkyne which was converted in the key synthetic step to the desired tetra-substituted alkene with regio- and stereo-control. Heteroaryl alkynes **17c-j** were synthesized from commercial heteroaryl halides **13c-j** as shown in Scheme 1. Heteroaryl halides **13c-j,** containing a free NH gave low yields in the Sonogashira coupling and so a variety of protecting groups were employed. Benzothiazolone **13c,** benzoxazolone **13d** and indole **13e** were protected with MOM, trityl and acetyl respectively to give **14c**, **14d** and **14e**. Meanwhile benzimidazole **13f**, benzotriazole **13g** and indazoles **13h-j** were protected with THP using 3,4-dihydro-2H-pyran and catalytic pyridinium *p*-toluenesulfonate to afford **14 h-j** in 56-89% yield.[9] In the case of benzimidazole **14f** and benzotriazole **14g**, a 1:1 mixture of THP-regioisomers was obtained. This mixture was used

without separation in the Sonagashira reaction, and then subsequently separated. Having suitably protected heteroaryl halides in hand, compounds **14c-j** were converted to alkynes **17c-j** via one of two routes. Initially for **17g-j**, a three step procedure was utilized. Coupling of **14g-j** and trimethylsilylacetylene under Sonogashira cross-coupling conditions[10] afforded alkynes **15g-j** which were then desilylated using potassium carbonate. Then, a base-mediated alkylation of terminal alkynes **16g-j** with ethyl iodide gave the desired internal alkynes **17g-j**. Later, a more efficient one pot procedure was used: halides **14c-f** were coupled with but-1-yn-1-yltrimethylsilane in the presence of palladium (II) acetate catalyst, 1,1'-bis(diphenylphosphino)ferrocene, copper iodide and cesium carbonate to afford the desired internal alkynes **17c-f** directly in 47-93% yields.

Scheme 1

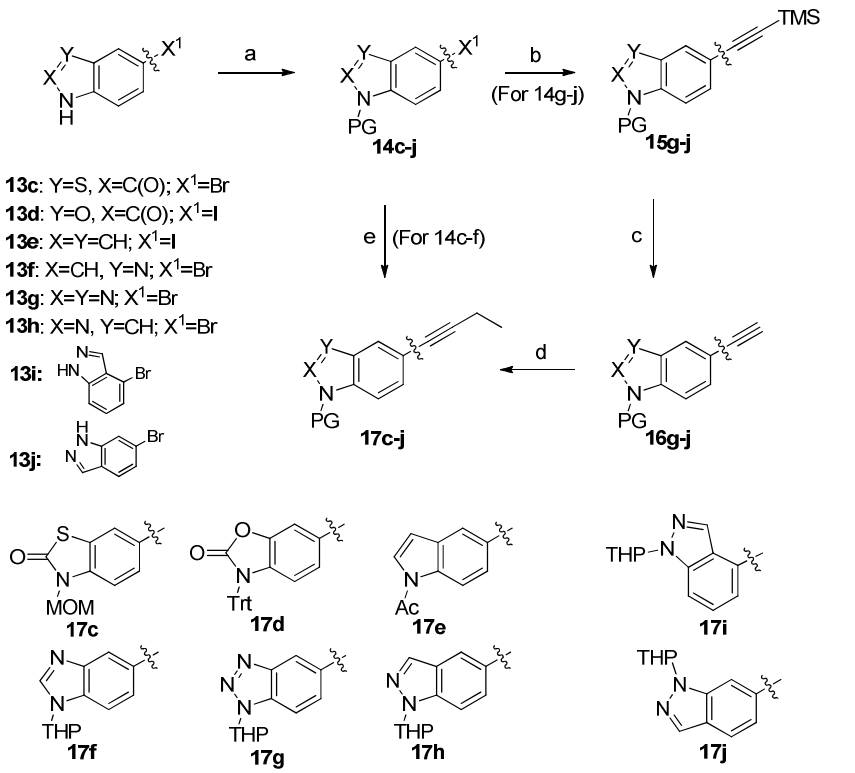

[a]Reagents and conditions: (a) For **13c**: MOM; MOM-Cl, K_2CO_3, DMF, 96%; **13d**: Tr-Cl, TEA, DCM, 83%; **13e**: Ac_2O, TEA, DMAP, DCE, 97%; **13f-j**: DHP, PPTS, DCM, 56-89%; (b) cat. $Pd(Ph_3P)_2Cl_2$,CuI, trimethylsilylacetylene, THF-TEA (5:1), 80 °C, 97-100%; (c) K_2CO_3, MeOH, rt, 49-98%; (d) n-BuLi, Et-I, THF/TMEDA (9:1), -78 °C-40 °C, 52-58%; (e) cat. $Pd(OAc)_2$, dppf, CuI, Cs_2CO_3, but-1-yn-1-yltrimethylsilane, DMA 80 °C, 47-93%.

In a similar way, alkynes **17a** and **17b** were synthesized from heteroaryl bromide **13a** or aryl bromide **13b** as shown in Scheme 2. Thus, bromopyridine **13a** was protected as the *N*-MOM intermediate in 40% yield, while sulfonamide **13b** was protected as the carbamate in 83% yield. Using Sonagashira cross-coupling conditions, both intermediates were converted to the alkynes **17a** and **17b** in 72-77% yield.

Scheme 2:

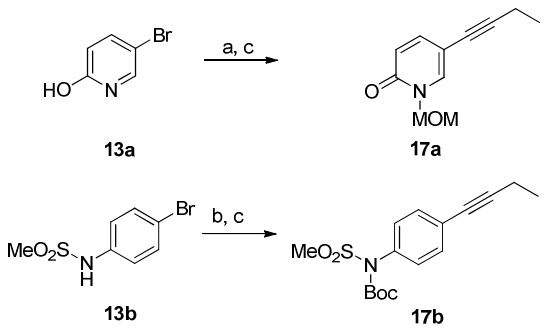

[a]Reagents and conditions: (a) MOM-Cl, K_2CO_3, DMF 40%; (b) Boc_2O, DMAP, DCM, 83%; (c) $Pd(OAc)_2$, dppf, CuI, Cs_2CO_3, but-1-yn-1-yltrimethylsilane 72-77%

To efficiently carry out structure-activity-relationship (SAR) studies, we utilized a regioselective, stereospecific, three-component coupling followed by deprotection and saponification to prepare final compounds **9c-h** (Scheme 3).[11] To this end, heteroaryl alkynes **17c-h**, iodobenzene and boronic acid **19** were coupled in 13-82% yield using catalytic $Pd(PhCN)_2Cl_2$ and K_2CO_3 in DMF-water. The tetra-substituted olefins **20c-h** were formed with good regioselectivity (typically >10: 1), and any undesired regioisomer and biaryl (derived from Suzuki coupling of **18** and **19**) side-products were removed by silica gel chromatography. The fully constructed tetra-substituted alkenes **20c-h** were then de-protected under acidic condition to give acrylic esters **21c-h** in high yield. Finally, the acrylic ester was hydrolyzed using lithium hydroxide to afford the acrylic acids **9c-h**. In an analogous way, alkynes **17a-b** and **17i-j** were converted to the respective final compounds **9a-b**, **9i-j**.

Scheme 3

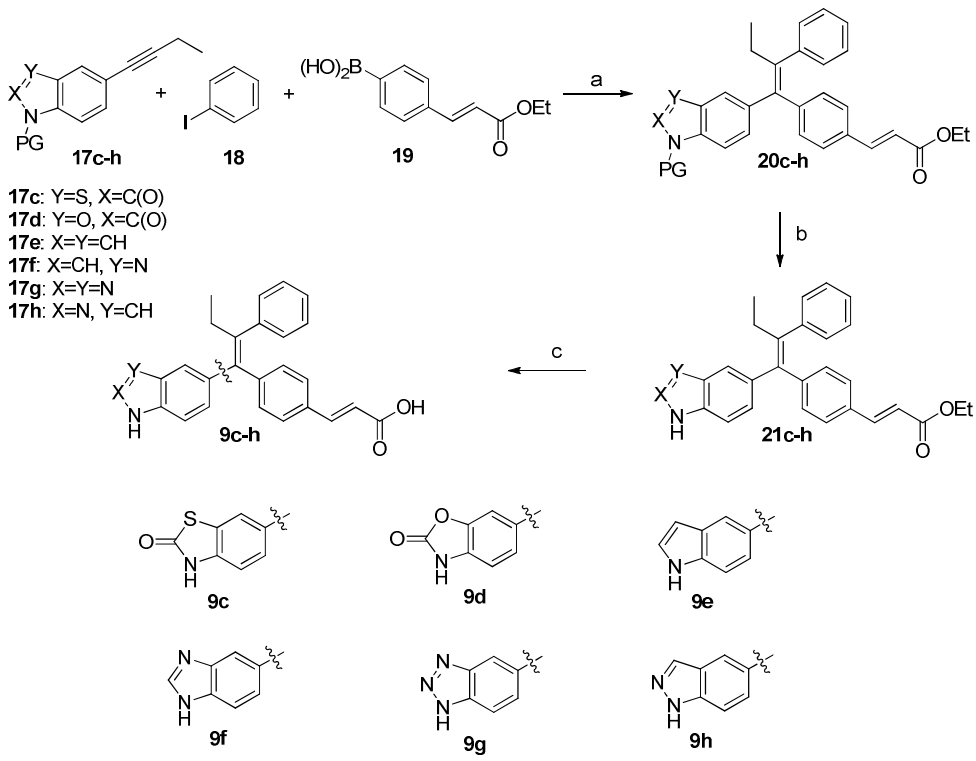

[a]Reagents and conditions: (a) cat. $Pd(PhCN)_2Cl_2$, K_2CO_3 , DMF/H_2O, 13-82%; (b) HCl, EtOH, 90-100%; (c) LiOH, THF-EtOH, 45-60%

To investigate substitution on the phenyl-linker region, compounds **10a-f** were prepared (Scheme 4) employing the same three-component coupling described in Scheme 3. Boronic acids **22** were used as coupling partners and afforded aryl aldehydes **23a-f** with good regioselectivity and moderate yields (30-68%). Aldehydes **23a-f** were then converted to (*E*)-acrylic esters **24a-f** via a Horner-Wadsworth-Emmons (HWE) reaction with triethylphosphonoacetate. Finally, compounds **10a-f** were obtained after removal of the THP protecting group and hydrolysis of the acrylic ester under standard conditions.

Scheme 4:

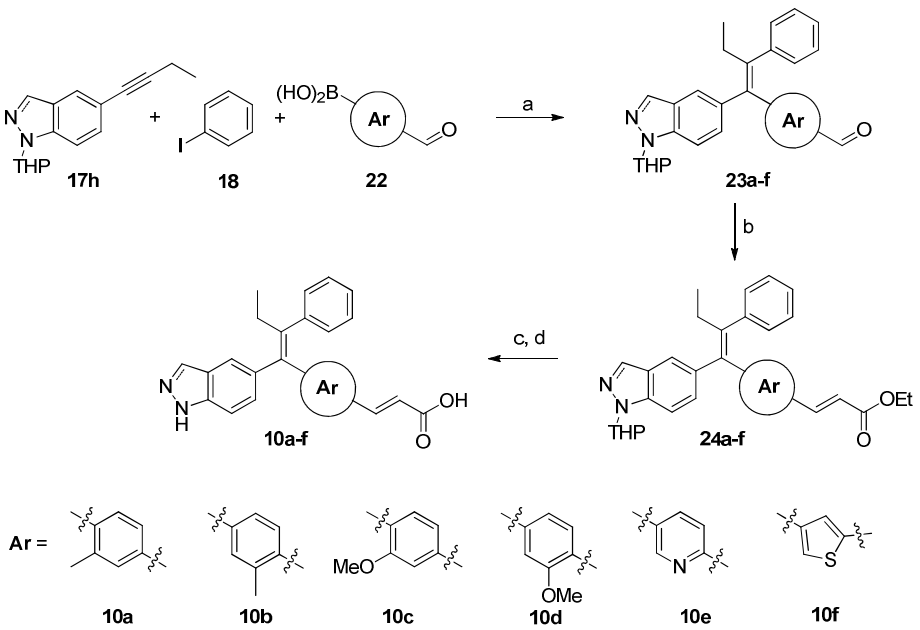

[a]Reagents and conditions: (a) cat. $Pd(PhCN)_2Cl_2$, K_2CO_3 , DMF/H_2O, 30-68%; (b) Triethylphosphonoacetate, LiCl, DBU, MeCN, 75-100%; (c) HCl, EtOH, 90-100%; (d) LiOH, THF-Et_2O, 54-60%

Compounds investigating substitution of the pendant phenyl ring were initially prepared (Scheme 5) using the three-component coupling described above. However for systems with an ortho-subtituent (i.e.**11a**) and/or an electron with-drawing substituent (i.e. **11e**), these coupling conditions gave poor yields (< 30%), or in some cases did not work due to the competing Suzuki cross-coupling of aryl iodide **25** and boronic acid **19**. Despite its inefficiency this chemistry was used to produce intermediates **26a-i** in 8-62% yield. Removal of the THP group and hydrolysis of the ester gave the desired compounds **11a-i** in good yields.

Scheme 5:

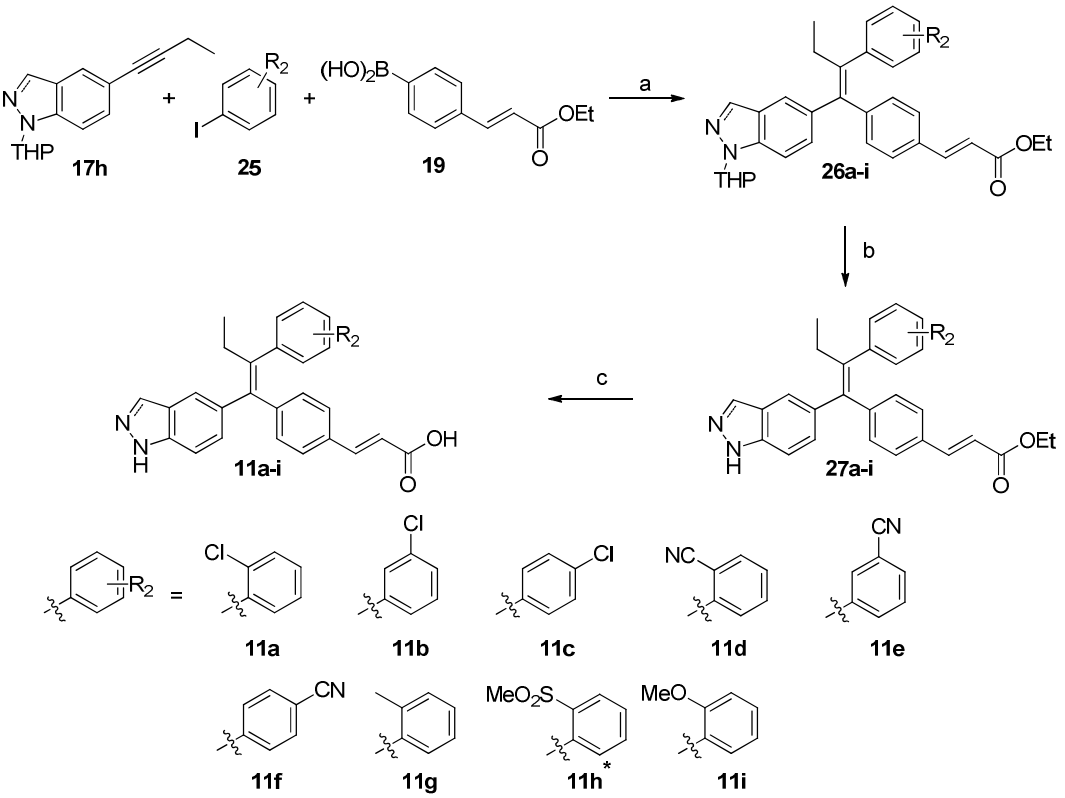

[a]Reagents and conditions: (a) cat. $Pd(PhCN)_2Cl_2$, K_2CO_3, DMF/H_2O, 8-62%; (b) HCl, EtOH, 95-100%; (c) LiOH, THF-EtOH, 11-77%; *2-iodothioanisole (**25**) was used in step (a) followed by oxone oxidation to give **26h**.

Alternate chemistry was used for the efficient synthesis of tetra-substituted alkenes containing ortho-substituted and/or electron-deficient aryls and heteroaryls as outlined in Scheme 6. Alkyne **17h** was converted to bis(pinacolato)diboryl-alkene intermediate **28** in high yield,[12] and this intermediate was sufficiently stable to be stored for future synthesis. More typically, it was used immediately in a sequential bis-arylation to prepare the desired tetra-substituted alkene with high regio- and stereo-control and in good yields.[13] Thus, in a one pot reaction from **17h**, intermediate **28** (not isolated) was reacted with 4-iodo benzaldehyde **29** to give the intermediate aldehyde **30**, which was coupled with aryl halide **32** in the presence of catalytic $PdCl_2(PPh_3)_2$ and aqueous KOH to give intermediates **33a-e** and **33l** in 21-99% yield overall. These were then homologated using a HWE reaction to give **34a-e** and **34l**. It was observed that lower temperatures (0-25 ºC)

resulted in higher regio-control in the key arylation reaction, and that intermediate **30** could also be isolated and stored for future use. Alternatively, intermediate **28** was coupled with ethyl 3-(4-iodophenyl)acrylate **31** in the presence of $PdCl_2(PPh_3)_2$ and Cs_2CO_3, followed by coupling with **32** in the presence of $PdCl_2(PPh_3)_2$ and aqueous potassium carbonate, to provide tetra-substituted alkenes **34j-k**. Lastly, the protecting groups of compounds **34a-e** and **34j-l** were removed under standard conditions to afford the targeted acrylic acid analogs **11j-l** and **12a-e**.

Scheme 6:

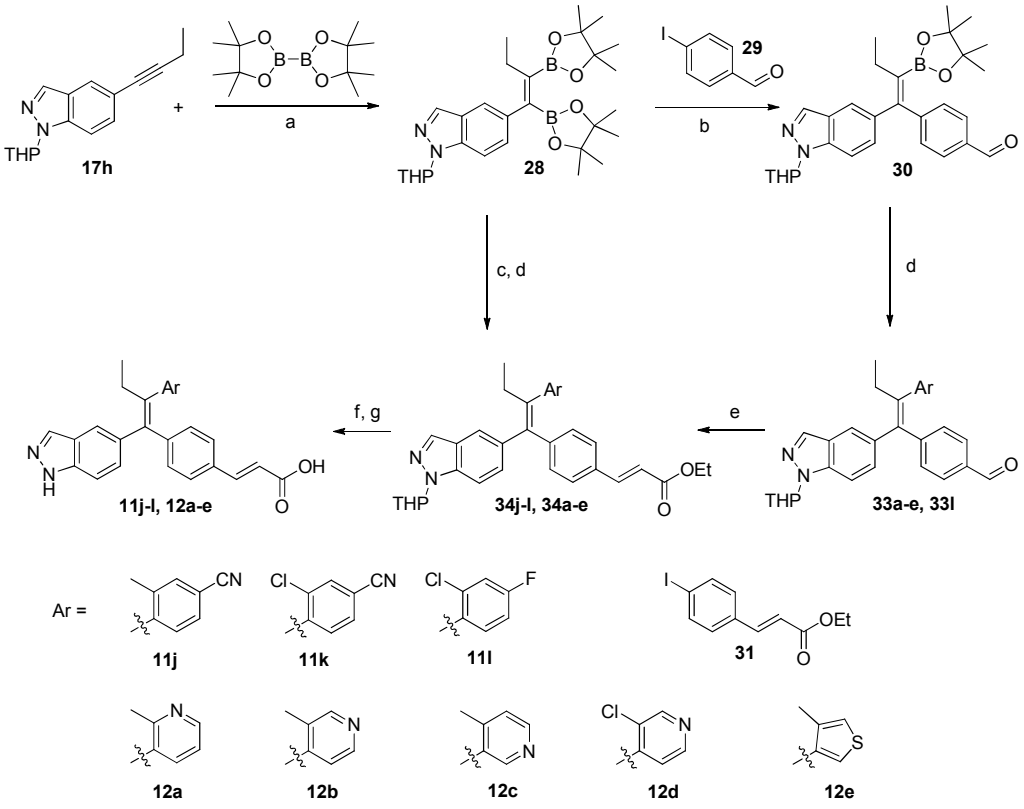

[a]Reagents and conditions: (a) cat. $Pt(PPh_3)_4$, bis(pinacolato)diboron, 2-MeTHF, 80 °C; (b) **29**, cat. $PdCl_2(PPh_3)_2$, Cs_2CO_3, 2-MeTHF, 0 °C-rt; (c) **31,** cat. $PdCl_2(PPh_3)_2$, Cs_2CO_3, 2-MeTHF, 0 °C-rt; (d) Ar-X **(32)**, cat. $PdCl_2(PPh_3)_2$, KOH (or K_2CO_3 in 1:1 2-MeTHF/DMSO), 2-MeTHF, reflux 21-99% (3 steps); (e) Triethyl-phosphonoacetate, LiCl, DBU, MeCN, rt, 56-96%; (f) HCl, EtOH; (g) LiOH, THF-EtOH, 26-93% (2 steps)

RESULTS AND DISCUSSION

In addition to more typical assays used in nuclear hormone receptor drug discovery programs such as binding and transcriptional assays, we also developed a cell based immunofluorescence assay (in-cell western assay, 'ICW') which monitored total ER-α protein levels in an MCF-7 breast cancer cell line. This assay was central to the program and was used to drive SAR to maximize ER-α degradation (SERD efficacy) of our ligands. Figure 2 shows an example of the assay with benchmark compounds, including fulvestrant, which was used as an internal control in each run of the assay, and we report degradation efficacy of compounds as a percent of this fulvestrant control. It should be noted that a small percentage of the ER-α still remains after fulvestrant treatment. This may reflect an inaccessible ER-α population resistant to degradation such as a nuclear insoluble fraction that is revealed upon cell permeabilization and antibody interrogation.[14]

Figure 2: MCF-7 ER-α degradation assay[a]

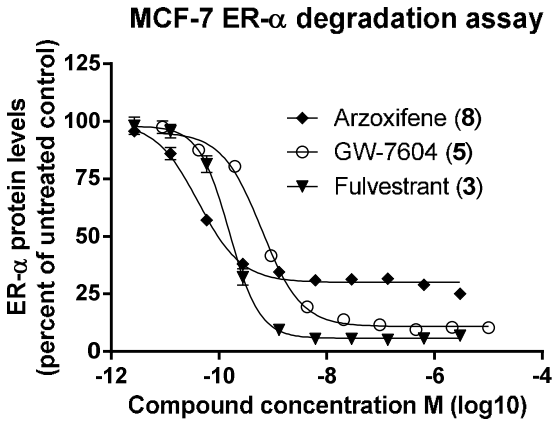

a: ER-α in-cell western in MCF-7 breast cancer cells in phenol-red free RPMI medium containing 5% charcoal dextran treated FBS; readings taken after 4 hours incubation using a SP-1 anti-ER rabbit monoclonal antibody

Table 1 shows the profiles of the SERMs arzoxifene (discontinued following a phase 3 in patients with metastatic breast cancer)[15] and pipendoxifene (phase 2, discontinued for unknown reasons),[16] and the SERDs fulvestrant and GW-5638/7604 in the key ER-α degradation assay. A number of points are worth highlighting, first that arzoxifene, although potent in the ER-α degradation assay, has relatively poor degradation efficacy at 71% of the fulvestrant control. Secondly, GW-7604, the active metabolite of GW-5638, is much more potent than the parent in this ER-α degradation assay. At 91% of the fulvestrant control, GW-7604 is also an efficacious degrader of ER-α.

Table 1: MCF-7 ER-α degradation profile of ER modulators

Compound	MCF-7 ER-α Degradation[a]		
	EC_{50} (μM)	Maximum Efficacy	Efficacy % of control[b]
Fulvestrant (3)	0.0004	94%	100%
GW-5638 (4)	0.39	82%	90%
GW-7604 (5)	0.0017	86%	91%
Pipendoxifene (6)	0.0001	83%	87%
Arzoxifene (8)	0.0002	67%	71%

a: ER-α in-cell western in MCF-7 breast cancer cells in phenol-red free RPMI medium containing 5% charcoal dextran treated FBS; readings taken after 4 hours incubation using a SP-1 anti-ER rabbit monoclonal antibody b: Efficacy recorded as percent of efficacy of fulvestrant control.

For a prodrug strategy to be maximally effective, the active species should be efficiently produced in humans. When we examined the cross-species microsome profile of GW-5638, we found that in all species, the active metabolite GW-7604 was indeed produced, but the ratio varied between species (Table 2). For example in rat liver microsomes, 82% of GW-7604 was produced after a 4 hour incubation, while in human liver microsomes, only 16% of GW-7604 was produced. In addition, we found that another oxidative metabolite **5c** was produced in human liver microsomes (21% after 4 hours), and that it was 100-fold less potent an ER-α

degrader than GW-7604 (ERα-degradation EC_{50} = 0.113 μM). Further the exposure of GW-7604 in mice following dosing of the parent GW-5638 was found to be relatively low (dosing of 100 mg/kg of GW-5638, gave: AUC (GW-5638) = 137 μg.hr/mL, AUC (GW-7604) = 13 μg.hr/mL). Thus metabolism of GW-5638 to the desired active species GW-7604 is inefficient across species *in-vitro* and in mouse PK studies.

Table 2: Cross-species *in-vitro* liver microsome profile of GW-5638

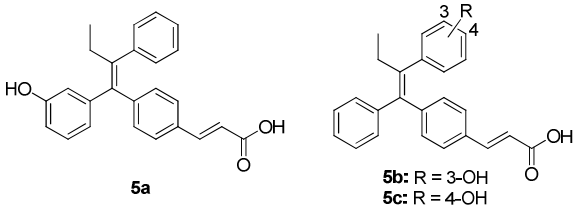

5a **5b:** R = 3-OH **5c:** R = 4-OH

Species	Compound detected (%)[a]				
	GW-5638 (4)	GW-7604 (5)	5a	5b	5c
Mouse	50	21	0	0	30
Rat	16	82	0	0	1
Dog	92	5	0	0	3
Human	63	16	0	0	21

a: Following 4 hours incubation in liver microsomes

We investigated a variety of scaffolds toward our goal of identifying fully efficacious ER-α degraders that had good exposure following oral dosing, and this paper will describe our investigation of the GW-5638 triphenylalkene scaffold. We initially explored the SAR in the region of the phenyl ring that is the site of metabolism of GW-5638 to the active 4-hydroxyphenyl metabolite, GW-7604 (Table 3).

Table 3: SAR of the phenol region of the triphenylalkene scaffold

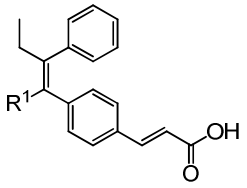

Compound	R^1	ER-α Degradation[a]		MCF-7 Viability[b]
		EC_{50} (μM)	Efficacy[c]	IC_{50} (μM)
4 (GW-5638)	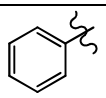	0.39	90%	0.985
5 (GW-7604)	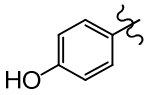	0.0017	91%	0.005
9a	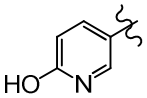	6.28	ND[d]	ND
9b	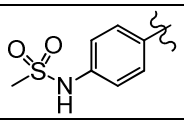	1.05	ND[d]	2.31
9c	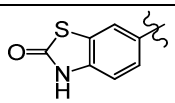	0.101	92%	0.158
9d	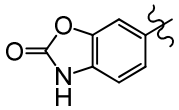	0.023	90%	0.056
9e	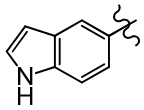	0.003	93%	0.009
9f	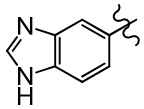	0.957	ND[d]	1.18
9g	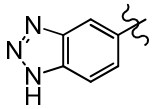	0.014	92%	0.053
9h	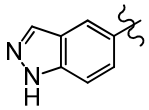	0.003	90%	0.006
9i	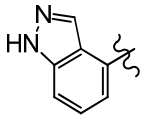	0.006	92%	0.021
9j	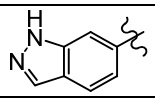	0.357	ND[d]	0.57

a: ER-α in-cell western in MCF-7 breast cancer cells in phenol-red free RPMI medium containing 5% charcoal dextran treated FBS; readings taken after 4 hours incubation using a SP-1 anti-ER rabbit monoclonal antibody b: MCF-7 viability assay in RPMI medium containing 10% FBS;

5 day incubation c: Efficacy recorded as percent of efficacy of fulvestrant control d: Not determined due to incomplete floor of dose response curve because of relative low potency of compound

Single ring systems such as pyridyl **9a** and sulfonamide **9b**, both lost a considerable amount of activity (> 1μM in the ER-α degradation assay) compared to **GW-7604** (EC_{50} = 0.0017 μM), potentially due to the high polarity of these moieties and/or the pyridone nature of **9a**. However when we examined bicyclic heterocycles such as the benzothiazolone **9c** and benzoxazolone **9d**, where a weakly acidic N-H exists in the cyclic structure (pKa 8.7),[17] improved activity was observed. Exploration of [6,5] systems improved the potency further; thus indole **9e** (EC_{50} = 0.003 μM), benzotriazole **9g** (EC_{50} = 0.014 μM) and indazole **9h** (EC_{50} = 0.003 μM) were high potency compounds, with the indole and indazole effectively equipotent to **GW-7604**. In contrast to these systems, basic benzimidazole **9f** was considerably less active (EC_{50} = 0.957 μM). In addition to good potency, indazole **9h** was also an efficacious ER-α degrader (90% of the fulvestrant control), and importantly delivered good exposure in mice following oral dosing (100 mpk po: AUC = 240 μg.hr/mL versus **GW-7604** AUC = 13 μg.hr/mL, from 100 mpk po dosing of **GW-5638**).

The importance of the directionality of the indazole N-H was highlighted when different isomers of **9h** were prepared. Thus the 4-indazole **9i** (EC_{50} = 0.006 μM), maintained potency compared to **9h**, while the 6-indazole isomer **9j** lost >100x potency (EC_{50} = 0.357 μM), presumably as it is unable to form the key hydrogen bond in the ligand binding domain of the estrogen receptor that **9h** is able to. Of note, all potent compounds were efficacious ER-α degraders, achieving ≥ 90% of the efficacy of the fulvestrant control. This was found to be the case in general for the triphenylalkene scaffold derivatives that contained the acrylic acid side-chain. The potency in an

MCF-7 breast cancer cell viability assay generally tracked with the ER-α degradation EC_{50}, with **9h** and **9e** both having an $IC_{50} < 0.010$ μM in this viability assay. With the identification of indazole **9h** as a potent, efficacious SERD, we proceeded to examine the SAR of the phenyl linker region of the scaffold (Table 4).

Table 4: SAR in the phenyl linker region of the triphenylalkene scaffold

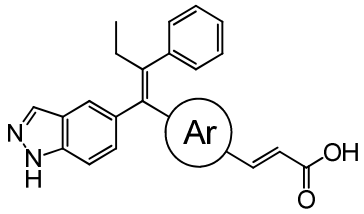

Compound	Ar	ER-α Degradation[a]		MCF-7 Viability[b]
		EC_{50} (μM)	Efficacy[c]	IC_{50} (μM)
9h	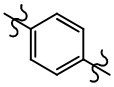	0.003	90%	0.006
10a	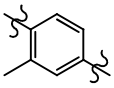	0.015	92%	0.036
10b	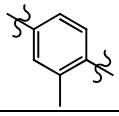	0.006	90%	0.014
10c	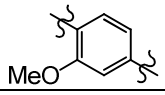	0.004	90%	0.012
10d	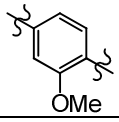	0.011	85%	0.031
10e	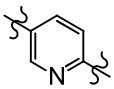	0.11	85%	0.21
10f	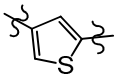	1.13	ND[d]	2.9

a: ER-α in-cell western in MCF-7 breast cancer cells in phenol-red free RPMI medium containing 5% charcoal dextran treated FBS; readings taken after 4 hours incubation using a SP-1 anti-ER rabbit monoclonal antibody b: MCF-7 viability assay RPMI medium containing 10% FBS; 5

day incubation c: Efficacy recorded as percent of efficacy of fulvestrant control d: Not determined due to incomplete floor of dose response curve because of relative low potency of compound

Although introduction of a methyl or methoxy substituent at either the 'internal' (**10a**, **10c**) or 'external' (**10b**, **10d**) positions relative to the core was tolerated, it did not lead to an increase in potency. Replacement of the phenyl ring with a heterocycle such as pyridine **10e** and thiophene **10f** led to a substantial drop-off in potency, indicating that these heterocyclic rings are not well tolerated in this region. It is interesting that **10d** is one of the few potent acrylic acid examples where a reduction of degradation efficacy was observed in the ER-α in-cell western assay. This suggests the importance of this region for maximal ER-α degradation efficacy, and may reflect the ability of the methoxy substituent to modulate the pKa of the key acrylic acid moiety.

In general, nuclear hormone receptor ligands, such as estradiol are lipophilic in nature,[18] and so introduction of polar groups while maintaining potency can be difficult. Throughout the program we explored typical lipophilic groups as well as trying to incorporate heteroatoms in the series, and Tables 5 and 6 show some of the SAR that was carried out on the pendent phenyl ring of indazole **9h** toward this goal.

Table 5: SAR of the pendent phenyl ring

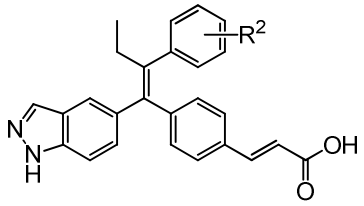

Compound	R^2	ER-α Degradation[a]	MCF-7 Viability[b]

		EC_{50} (μM)	Efficacy[c]	IC_{50} (μM)
9h	H	0.003	90%	0.006
11a	o-Cl	0.0007	92%	0.002
11b	m-Cl	0.002	91%	0.012
11c	p-Cl	0.010	93%	0.015
11d	o-CN	0.003	93%	0.012
11e	m-CN	0.028	87%	0.100
11f	p-CN	0.036	93%	0.047
11g	o-Me	0.0008	92%	0.004
11h	o-SO_2Me	0.049	91%	0.070
11i	o-OMe	0.004	93%	0.025
11j	o-Me, p-CN	0.001	89%	0.005
11k	o-Cl, p-CN	0.0009	92%	0.004
11l	o-Cl, p-F	0.0007	91%	0.002

a: ER-α in-cell western in MCF-7 breast cancer cells in phenol-red free RPMI medium containing 5% charcoal dextran treated FBS; readings taken after 4 hours incubation using a SP-1 anti-ER rabbit monoclonal antibody b: MCF-7 viability assay in RPMI medium containing 10% FBS; 5 day incubation c: Efficacy recorded as percent of efficacy of fulvestrant control

Table 5 shows that substitution at the ortho position (**11a**, **11d**) is preferred over the *meta*- or *para*-position (**11c**, **11e**, **11f**) for both a more polar substituent (-CN) or a lipophilic substituent (-Cl). Of note, ortho-chloro **11a**, gives a 3-5 fold increase in potency over the unsubstituted phenyl **9h**, while ortho-nitrile **11d** is equipotent to **9h**. Additional substituents were examined at the ortho-position, with a strongly polar ortho-sulfone substituent leading to a drop off in activity i.e. compare **11h** (ER-α degradation EC_{50} = 0.049 μM) to ortho-methyl **11g** (ER-α degradation EC_{50} = 0.0008 μM). We found that adding an ortho-methyl or ortho-chloro substituent to otherwise less active derivatives (such as the para-cyano derivative **11f**; ER-α degradation EC_{50} = 0.036 μM), resulting in disubstituted systems such as **11j** and **11k**, gave a substantial 30-fold increase in potency (**11j** and **11k**: ER-α degradation $EC_{50} \leq 0.001$ μM). The ortho-chloro, para-fluoro derivative **11l** was also a high potency compound. We also found that heterocycles could be incorporated in this region (Table 6). The 4-pyridyl **12b** (ER-α degradation EC_{50} = 0.008 μM)

being the preferred substitution pattern compared to **12a** and **12c** (ER-α degradation EC_{50} > 0.10 μM). Chloro-pyridyl **12d** and thiophene **12e** were also potent heterocyclic compounds in this region. As with SAR on the indazole region, potency in the ER-α degradation assay generally tracked with the MCF-7 breast cancer cell viability IC_{50}, with compounds such as **11a**, **11k**, **11l** and **12d** all having an IC_{50} < 0.005 μM.

Table 6: Select pendant heterocycles are tolerated

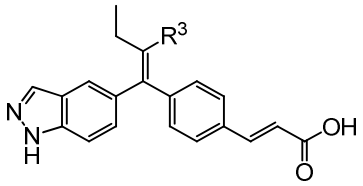

Compound	R^3	ER-α Degradation[a]		MCF-7 Viability[b]
		EC_{50} (μM)	Efficacy[c]	IC_{50} (μM)
11g		0.0008	92%	0.004
12a		0.16	ND[d]	0.20
12b	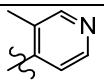	0.008	89%	0.016
12c	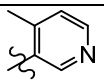	0.11	91%	0.15
12d	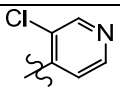	0.002	90%	0.004
12e	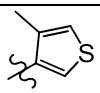	0.0005	90%	0.002

a: ER-α in-cell western in MCF-7 breast cancer cells in phenol-red free RPMI medium containing 5% charcoal dextran treated FBS; readings taken after 4 hours incubation using a SP-1 anti-ER rabbit monoclonal antibody b: MCF-7 viability assay in RPMI medium containing 10% FBS; 5 day incubation c: Efficacy recorded as percent of efficacy of fulvestrant control d: Not determined due to incomplete floor of dose response curve because of relative low potency of compound

As illustrated in Tables 3-6, a number of potent and efficacious ER-α degraders were identified. In order to quickly determine those that had good exposure and activity following oral dosing, we heavily utilized a 4-day immature rat uterine wet weight assay, which allowed rapid determination of compound antagonist activity in an ER responsive tissue (immature rat uterus) while competing against the native ER ligand estradiol (i.e. antagonist mode).[19] Drug plasma levels were also obtained from this assay. Table 7 shows the reduction in immature rat uterine weight for select compounds when compared to estradiol-only treated animals (the table also includes exposure in mice from separate PK studies).

Table 7: Immature rat uterine wet weight assay (antagonist mode) and mouse pharmacokinetics

		Rat Uterine Wet Weight[a]		**Mouse PK**
Cpd	**ER-α Degradation EC_{50} (μM)**	**Percent inhibition[b]**	**Drug levels (nM)[c]**	**po AUC (μg.hr/mL)**
9d	0.023	28%	0.2	3.0
9e	0.003	47%	ND	9.4
9g	0.014	15%	ND	2.3
9h	0.003	69%	3.8	5.8

9i	0.006	35%	0.1	2.8
11a	0.0007	82%	3.7	15
11b	0.002	81%	11	11
11d	0.003	27%	ND	0.2
11g	0.0008	72%	1.7	7.2
11j	0.001	48%	14[d]	4.3
11k	0.0009	60%	10[d]	2.9
11l	0.0007	81%	5.2	8.8
12b	0.008	7%	7.6	0.081
12d	0.002	66%	0.5	0.11
12e	0.0005	105%[e]	10	3.8

a: Compounds administered orally (1 mg/kg po) followed by an oral dose of 0.1 mg/kg ethynyl estradiol each day for 3 days. On the fourth day, 24 hours post dose, the animals were euthanized and the uterus was removed and weighed. Plasma was taken at the time point indicated. b: 100 x [($Vehicle_{EE}$ – Cpd)/($Vehicle_{EE}$ – Vehicle)], where '$Vehicle_{EE}$' is the uterine wet weight of the of the vehicle animals dosed with ethynyl estradiol (0.1 mg/kg); 'Cpd' is the uterine wet weight of the of the compound treated animals dosed with ethynyl estradiol (0.1 mg/kg); 'Vehicle' is the uterine wet weight of the of the vehicle animals c: Measured at 24 hrs after last dose unless otherwise indicated d: Measured at 6 hrs after last dose e: In same assay, **11l** = 112%

In general, compounds that effectively antagonized estradiol-induced uterine weight gain (>75% compared to vehicle) when dosed at 1 mg/kg orally, had good potency in the ER-α degradation assay (EC_{50} <0.001 μM) and also had measurable drug levels at the end of the study (C_{24} > 3 nM following a 1mg/kg po dose). In this way, the uterine assay identified promising compounds such as **11a**, **11l** and **12e**, while de-emphasizing otherwise potent *in-vitro* compounds such as indole **9e** or indazole **9i**. Although **12e** demonstrated robust activity in the UWW model, it had lower exposure in mouse PK (mouse po AUC @ 10 mg/kg = 3.8 μg.hr/mL) than **11a** and **11l** (mouse po AUC @ 10 mg/kg = 15 μg.hr/mL and 8.8 μg.hr/mL respectively). In addition, the presence of a thiophene in **12e** was of concern due to the potential for reactive metabolite formation *in-vivo*, and so we did not pursue **12e** further.[20] Compounds **11a** and **11l** had a similar *in-vitro* and uterine assay profile, and were subsequently profiled in additional assays including a tamoxifen-resistant MCF-7 xenograft model. Ultimately **11l** was selected for development and Table 8 shows a comparison to clinical benchmarks. **11l** is a potent ER-α binder (IC_{50} = 6.1 nM), a full transcriptional antagonist with no agonism (3x ERE, IC_{50} = 2 nM), and displays good potency and efficacy in ER-α degradation (EC_{50} = 0.7 nM) and MCF-7 breast cancer cell viability (IC_{50} = 2.5 nM) assays.

Table 8: 11l shows a favorable *in-vitro* profile compared to benchmark compounds

Compound	Binding (nM)[a]		Transcriptional Antagonism[b]	ER-α Degradation[c]		MCF-7 Viability[d]	
	ER-α IC_{50}	ER-β IC_{50}	IC_{50} (nM)	EC_{50} (nM)	Efficacy[e]	IC_{50} (nM)	Efficacy[e]
11l	6.1	8.8	2.0	0.7	91%	2.5	99%
Fulvestrant (3)	24	21	0.6	0.4	100%	0.6	100%
GW-7604 (5)	6.0	3.0	18	1.8	91%	5.0	98%
Pipendoxifene (6)	ND	ND	0.6	0.1	87%	0.4	89%
Arzoxifene (8)	42	240	0.3	0.2	71%	0.4	73%

a: Competitive radiometric binding in TEGM ; 2.5 nM ER-α or 1.5 nM ER-β, 1.5 nM ^{3}H-E2. b: 3X ERE-TK-Luc reporter vector, phenol-red free RPMI containing 10% charcoal dextran treated FBS plus 17β-estradiol (0.1 nM), 24 hrs. c: ER-α in-cell western in MCF-7 breast cancer cells in phenol-red free RPMI medium containing 5% charcoal dextran treated FBS; readings taken after 4 hours incubation using a SP-1 anti-ER rabbit monoclonal antibody d: MCF-7 viability assay in RPMI medium containing 10% FBS; 5 day incubation e: Efficacy recorded as percent of efficacy of fulvestrant control

Of particular note are the optimized levels of ER-α degradation for **11l** (91%) compared to arzoxifene (**8**) (71%) and pipendoxifene (**6**) (87%) and that these efficacy levels translate into increased efficacy in the MCF-7 viability assay (**11l**: 99% efficacy; 4; arzoxifene (**8**): 73% efficacy; pipendoxifene (**6**): 89% efficacy). Indeed, we observed a correlation between ER-α degradation efficacy and MCF7-viability efficacy which extended across chemical scaffolds and is captured graphically in Figure 3. Although not definitively causative, this correlation indicates that optimization of ER-α degradation efficacy leads to compounds with improved efficacy in a breast cancer cell viability assay. As will be presented below, this increase in *in-vitro* efficacy also led to improved efficacy in a xenograft model of tamoxifen-resistance.

Figure 3: Optimization of efficacy in the ER-α degradation assay correlates with increased efficacy in the MCF-7 breast cancer cell line viability assay

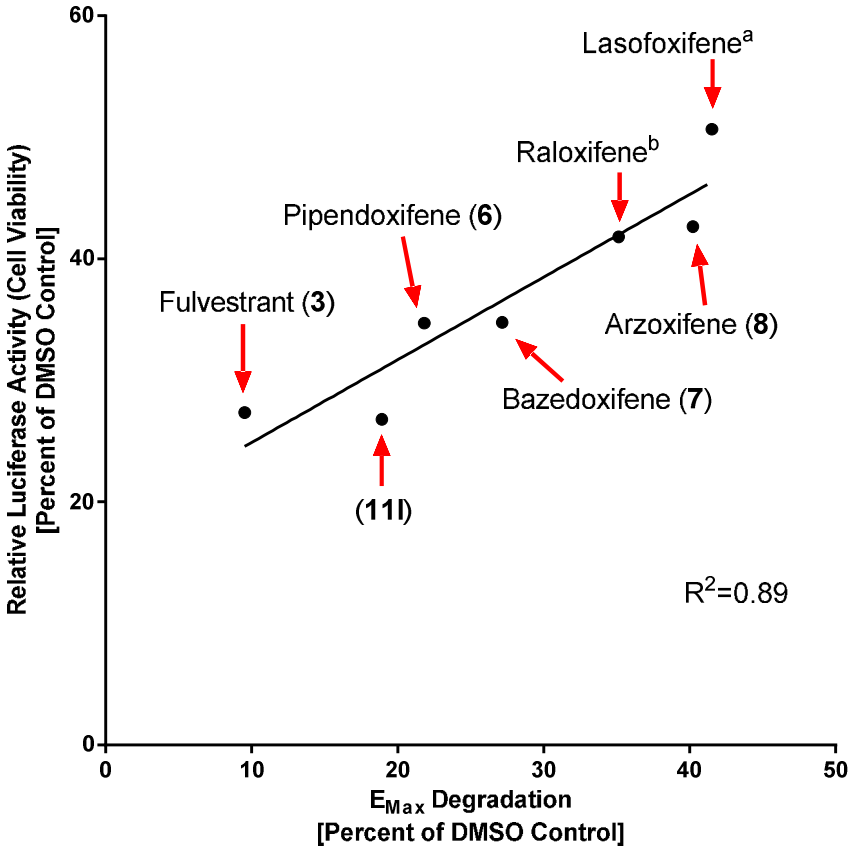

[a]: SERM for osteoporosis;[21] [b]: SERM for osteoporosis[22]

The robust degradation of **11l** in the in cell western assay was confirmed in a western blot assay as shown in Figure 4. Similar to fulvestrant, **11l** displays robust degradation of ER-α in this assay format. Of note is that, although an agonist, estradiol also leads to degradation of ER-α, while 4-hydroxytamoxifen (**2**) as is known the literature, leads to stabilization of ER-α (an increase in protein levels).

Figure 4: Western blot analysis confirms **11l** is a robust degrader of ER-α[a]

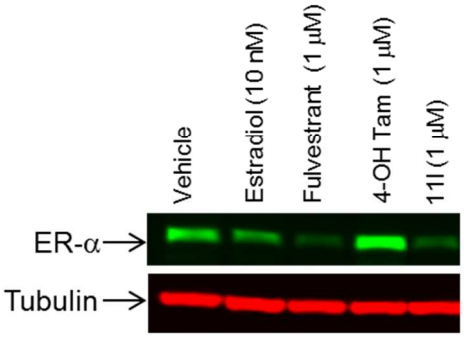

a: MCF-7 cells in RPMI supplemented with 10% charcoal dextran treated FBS; compound treatment for 20 hours, cell lysates separated electrophoretically using NuPAGE 4-12% Bis Tris Gels; SP-1 anti-ERα antibody and imaged using a LI-COR Odyssey infrared imaging system.

The pharmacokinetic profile of **11l** (Table 9) shows it is a low clearance molecule across species, with good bioavailability (40-60%). As would be expected for a lipophilic carboxylic acid, the compound is highly bound to plasma proteins (>99.5% across species), and has a low to moderate volume of distribution (V_{ss} = 0.2 to 2.0 L/Kg across species).

Table 9: Cross species pharmacokinetic of **11l** [a]

Species	**CL (mL/min/kg)**	**V_{ss} (L/kg)**	**$t_{1/2}$ (iv) (hr)**	**C_{max} (Oral) (μg/mL)**	**AUC (Oral) (μg·hr/mL)**	**Oral %F**
Mouse	11	1.2	4.2	4.4	8.8	61
Rat	14	1.9	3.9	1.8	5.8	49
Dog	1.6	0.2	11	20	69	61
Cyno	7.0	0.5	13	6.1	10	42

a: Dosed intravenously at 3 mg/kg and per orally at 10 mg/kg in PEG400 / PVP / TW80 / 0.5% CMC in water, 9:0.5:0.5:90

Metabolism profiling of **11l** conducted in microsomes, with phase 1 and phase 2 cofactors added, showed the acyl glucuronide to be the major metabolite across species. The stability of this acyl glucuronide in physiological medium (pH 7.4 phosphate buffer at 37ºC) was examined to understand its potential for reactivity (Figure 5).[23]

Figure 5: Percent remaining of **11l** acyl glucuronide in pH 7.4 phosphate buffer at 37 °C

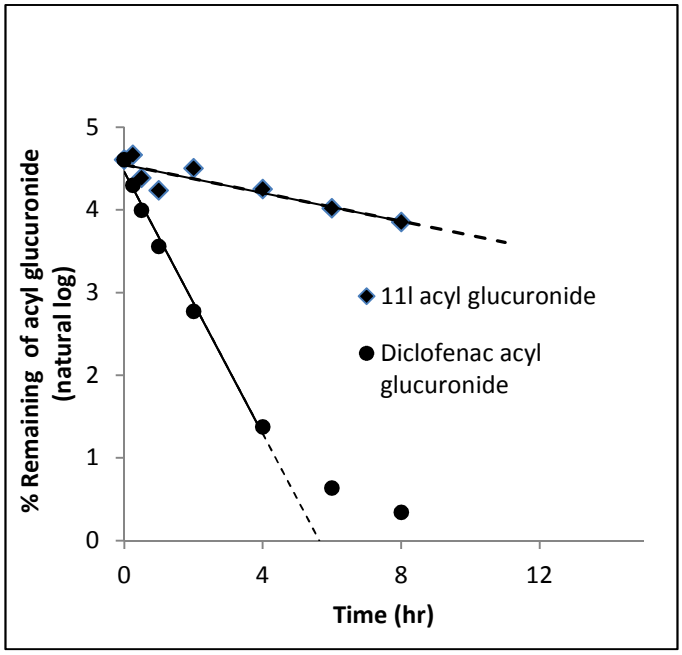

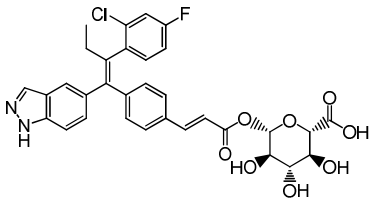

11l Acyl glucuronide

Compared to the diclofenac O-glucuronide positive control ($t_{1/2}$ = 0.9 hr), the stability of the **11l** O-glucuronide was good at $t_{1/2}$ = 8.1 hr, leading to the conclusion that the potential risk for idiosyncratic toxicity of **11l** was low. Cytochrome P450 inhibition profiling of **11l** indicated it had little to no inhibition against CYP1A2, CYP2D6 or CYP3A4 (IC_{50} > 20 μM), modest inhibitory effect on CYP2C9 and CYP2C19 (IC_{50} = 2.2 μM and 3.3 μM respectively), and potent inhibition of CYP2C8 (IC_{50} of < 0.1 μM). Inhibition of CYP2C8 was not considered a major liability as few therapeutics are metabolized exclusively by CYP2C8, suggesting the potential for drug-drug interactions is low.[24]

Selectivity of **11l** over other nuclear hormone receptors was found to be good. In transcriptional reporter assays for the mineralocorticoid (MR), progesterone-A (PR-A), progesterone-B (PR-B) and glucocorticoid (GR) receptors, **11l** had minimal activity (IC_{50} > 1 μM). While in binding assays, **11l** displayed little activity towards the androgen receptor (AR; IC_{50} > 4 μM) and GR (IC_{50} = 0.99 μM). In a CEREP panel of radioligand binding assays for 54 diverse targets (protein-free conditions), **11l** at 10 μM displayed >50% binding to 7 targets. However, the only appreciable activity seen in cell-based functional assays for these 7 targets was for the GABA-gated chloride channel (IC_{50} = 1.1 μM) and the dopamine transporter (IC_{50} = 3.4 μM). In light of the high plasma protein binding of **11l**, these low micromolar activities were not considered an issue as selectivity for the estrogen receptor is >500 fold (MCF-7 viability = 2 nM; ER-α degradation = 0.7 nM). **11l** produced no significant inhibition of hERG current at doses up to 30 μM in a patch clamp assay, and was Ames negative in the TA-98 and TA-100 tester strains.

Compound **11l** was extensively characterized in xenograft models of breast cancer. In these models supplemental estradiol (E2) is used to drive xenograft tumor growth *in-vivo* (in the form of an implanted slow-release pellet), and these high E2 ligand concentrations (300-400 pg/ml) require higher concentrations of **11l** in order to out-compete the native ligand (E2) and so mediate an inhibitory effect. This is of relevance as plasma E2 levels in the target patient population of post-menopausal women (~5 pg/mL)[25] are substantially lower than those of the various pre-clinical models. Thus pre-clinical models run in the context of high E2 plasma concentrations likely significantly overestimate **11l** dose and plasma levels necessary to drive efficacy in a post-menopausal setting.

Figure 6 shows the robust activity of **11l** in a tamoxifen-sensitive MCF-7 xenograft model, with 3 mg/kg/day dosed orally showing substantial tumor-growth inhibition, while at the highest dose of 100 mg/kg/day, all animals showed tumor regression of more than 50%. No weight loss was observed. Fulvestrant was run as a positive control in this assay at a dose of 200 mg/kg sub-cutaneously 3x per week, and caused only tumor stasis. The mediocre activity of fulvestrant in this and other xenograft models is not due to an insufficient exposure, as this regimen produces sustained fulvestrant levels that are 30-fold greater than those obtained in the clinic (fulvestrant xenograft C_{max}~ 0.75 ng/mL and C_{min} ~0.45 ng/mL versus clinical C_{max} = 0.028 ng/mL and C_{min} ~0.012 ng/mL).[26]

Figure 6: 11l shows robust dose-responsive activity in a tamoxifen-sensitive MCF-7 xenograft model[a]

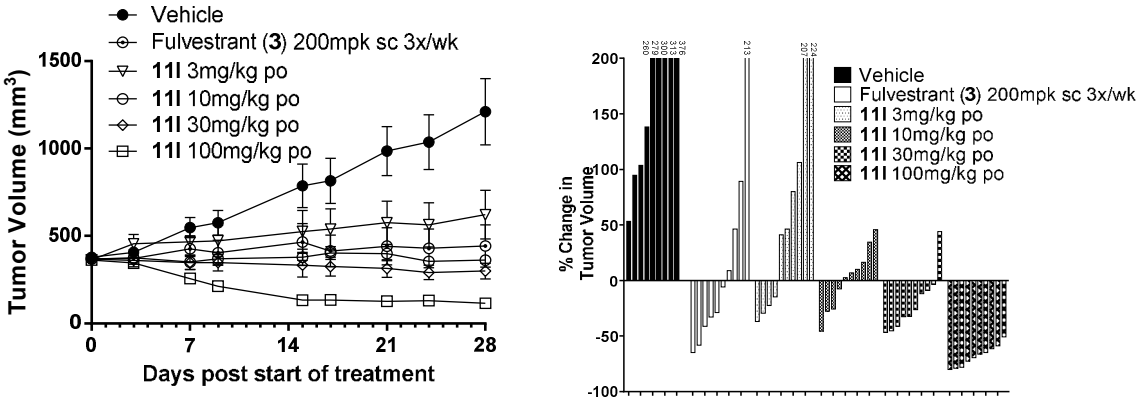

a: MCF-7 tamoxifen-sensitive xenograft in nu/nu mice using subcutaneous 0.72 mg estradiol pellets. MCF-7 cells subcutaneously injected 2-3 days post pellet implantation. *n* = 9-10 animals per group; Tumor volume (length x width^2/2) was monitored weekly. Animals were treated with vehicle or compound daily. Left panel shows tumor growth time course; right panel shows individual tumor volume on day 28.

Continued dosing of **11l** to the 100 mg/kg/day cohort in this model beyond the initial 28 days produced a durable response with a median time to progression for **11l** of >1 year. In contrast, emergence of resistance with tamoxifen occurred at about 70 days, clearly showing the differential profile of **11l**.

The initial target patient population for the SERD program is women who have progressed on endocrine therapy such as tamoxifen. To mimic this pre-clinically, we developed models of endocrine resistance by continuous dosing of tamoxifen to mice in an MCF-7 xenograft until tumor re-growth occurred. These individual tumors that were resistant were then propagated in the presence of tamoxifen and used as the source material for tamoxifen-resistant xenograft studies. Figure 7 illustrates the activity of **11l** in this tamoxifen-resistant setting compared to fulvestrant (**3**), pipendoxifene (**6**) and arzoxifene (**8**). Compound **11l** showed robust activity, with a dose of 30 mg/kg giving tumor stasis (tumor volume fold over start = 1.1), and all tumors regressing at 100 mg/kg (tumor volume fold over start = 0.34). Fulvestrant and pipendoxifene showed only tumor-growth inhibition (tumor volume fold over start = 2.1 and 1.8 respectively), while arzoxifene had no inhibitory activity compared to vehicle (tumor volume fold over start = 3.3).[27] The poor performance of arzoxifene in the tamoxifen-resistant setting is noteworthy considering that it is more potent than **11l** in the ER-α degradation and viability assays (Table 8), and has equivalent exposure to **11l** on day 28 of the xenograft study (arzoxifene AUC_{day28} = 50 μg.hr/mL; **11l** AUC_{day28} = 45 μg.hr/mL). Of note is that arzoxifene has poor *efficacy* in the ER-α degradation assay compared to **11l** (ER-α degradation efficacy: **11l** (91%) versus arzoxifene (71%)).

Figure 7: 11l shows robust activity in an MCF-7 tamoxifen-resistant xenograft model and is superior to benchmark compounds[a]

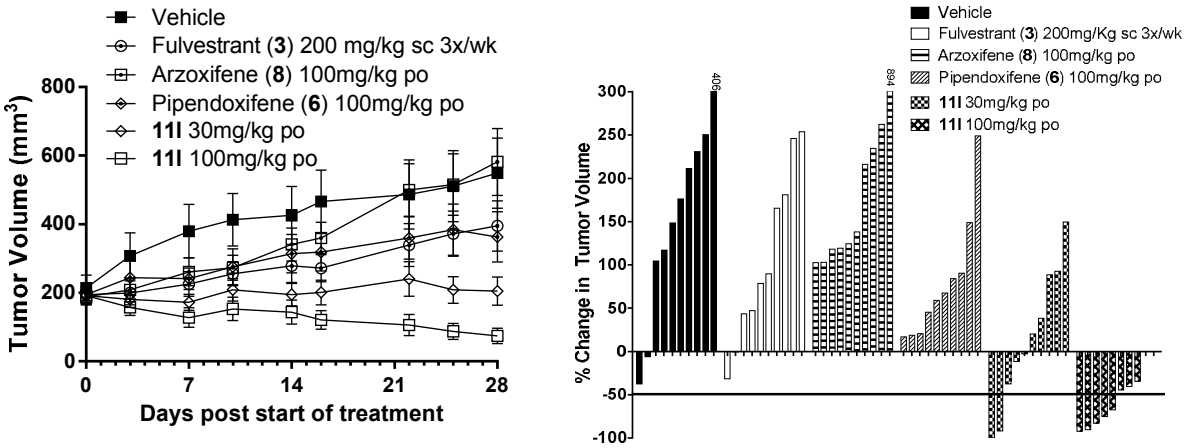

	Tamoxifen-resistant xenograft study		
Compound	**Dose (mg/kg)**	**Tumor Volume (Fold over start)**	**AUC_{day28} (μg.hr/mL)**
Vehicle	-	2.6	-
Fulvestrant	200 SC 3xwk	2.1	11
Pipendoxifene	100 po	1.8	7
Arzoxifene	100 po	3.3	50
11l	30 po	1.1	21
11l	100 po	0.34	45

a: MCF-7 tamoxifen-resistant xenograft in nu/nu mice using subcutaneous 0.72 mg estradiol pellets. *n* = 8-10 animals per group; Tumor volume (length x width^2/2) was monitored weekly. Animals were treated with vehicle or compound daily. Left panel shows tumor growth time course; right panel shows individual tumor volume on day 28.

The improved profile of **11l** over GW-5638 was clearly demonstrated in this MCF-7 tamoxifen-resistant xenograft setting where at a dose of 100 mg/kg po, GW-5638 only resulted in tumor growth inhibition (tumor volume fold over start = 2.6, separate experiment, data not shown) compared to tumor regression for **11l** at this dose (tumor volume fold over start = 0.34).

CONCLUSION

Through our SAR studies on a triphenylalkene scaffold, we identified a series of indazole ER-α modulators that exhibited a dual mode of action being both potent transcriptional antagonists and degraders of the estrogen receptor (SERDs). Importantly, the series of compounds in general, and the clinical candidate **11l** in particular are high efficacy degraders of the ER-α, reducing the levels of ER-α to a similar extent as fulvestrant. **11l** exhibited good bioavailability across species and displayed robust activity in tamoxifen-sensitive and tamoxifen-resistant xenograft models of breast cancer. Activity was superior to fulvestrant and other benchmark compounds in these studies. Compound **11l** (GDC-0810 or ARN-810) is currently in clinical trials in women with locally advanced or metastatic estrogen receptor-positive breast cancer.

EXPERIMENTAL SECTION

Supporting Information Available: Experimental procedures for all compounds and intermediates. This material is available free of charge via the Internet at http://pubs.acs.org

Experimental Procedures (Chemistry)

All air and moisture sensitive reactions were carried out under an inert atmosphere of nitrogen. All reactive liquid reagents were transferred by syringe or cannula and were added into the flask through a rubber septum. All other solvents and reagents were obtained from commercial sources and used as received unless otherwise stated. Both ^{1}H and ^{13}C spectra were obtained on a Bruker 400 spectrometer at 400 MHz and 100 MHz, respectively. Chemical shifts are reported in parts per million (δ) from an internal standard of residual DMSO (2.50 ppm or 39.5 ppm), methanol (3.31 ppm or 49.0 ppm), or chloroform (7.26 ppm or 77.2 ppm). Proton chemical shift data are reported as follows: chemical shift, multiplicity (s=singlet, d=doublet, t = triplet, q = quartet, m = multiplet, b = broad), integration, coupling constant (*J*) reported in hertz. Analytical thin-layer chromatography (TLC) was performed on commercial silica plates (Merck 60-F 254, 0.25 mm thickness); compounds were visualized by UV light (254 nm). All yields reported are not optimized. Normal phase purifications were performed on silica gel columns using a Biotage (SP1 or SP4), an ISCO Combiflash Companion XL or ISCO Combiflash Torrent using pre-packed silica gel columns. Reversed phase semipreparative HPLC purifications were carried out using a Shimadzu Discovery VP system with a SPD-20A prominence UV/vis detector (190-700 nm range). The columns used were a Waters SunFire C18 (19 mm x 150 mm) or a YMC-Pack Pro ODS-A (20 mm x 150 mm) or a Phenomenex, Luna 5 μ C18 semipreparative (250 x 10 mm) column with a acetonitrile-water solvent mixture in the presence of 0.1% TFA. The purity of target compounds was determined by ^{1}H NMR, analytical HPLC/MS and high resolution mass spectroscopy and shown to be > 95% pure prior to biological testing. Low-resolution mass spectra (LRMS) were recorded on a WatersMicromass ZQ using electrospray positive ionization.

High-resolution mass spectra (HRMS) were obtained on an Agilent ESI-TOF mass spectrometer using electrospray positive or negative ionization.

5-Bromo-1-(tetrahydro-2H-pyran-2-yl)-1H-indazole (14h)

A 250-mL round-bottom flask equipped with a magnetic stir bar, a rubber septum, and a N_2 inlet was charged with 5-bromo-1H-indazole (10 g, 50.7 mmol) and anhydrous dichloromethane (101 mL). To this solution, 3,4-dihydro-2H-pyran (23 mL, 253.8 mmol) was added in one portion at room temperature followed by addition of PPTS (1.28 g, 5 mmol). The resulting mixture was stirred at room temperature for 48 h. Upon completion by TLC (or LCMS), the reaction mixture was quenched with water and extracted with dichloromethane (3x100 mL). The combined organic extracts were washed with water (100 mL), washed with brine (50 mL), dried over sodium sulfate, filtered, concentrated, and purified by silica gel chromatography (0-10% ethyl acetate in hexanes) to give 5-bromo-1-(tetrahydro-2H-pyran-2-yl)-1H-indazole as a pale yellow oil (89% yield). ^{1}H NMR (400 MHz, DMSO-d_6): δ 8.10 (s, 1H), 8.00 (d, 1H, J = 1.85 Hz), 7.72 (d, 1H, J = 8.90 Hz), 7.53 (dd, 1H, J = 1.85 Hz, J = 8.90 Hz), 5.83 (dd, 1H, J = 2.60 Hz, J = 9.80 Hz), 3.89-3.83 (m, 1H), 3.75-3.69 (m, 1H), 2.43-2.31(m, 1H), 2.04-1.92 (m, 2H), 1.80-1.64 (m, 1H), 1.60-150 (m, 2H). ^{13}C NMR (100 MHz, DMSO-d_6): δ 137.9, 132.8, 128.9, 125.7, 123.2, 113.4, 112.4, 84.1, 66.5, 28.8, 24.7, 22.0.

Method B: General procedure for Sonagashira coupling of protected aryl or heteroaryl halides with but-1-yn-1-yltrimethylsilane

A mixture of the appropriate aryl or heteroaryl halide (1.0 equiv), Cs_2CO_3 (1.3-3.0 equiv), CuI (0.05-0.2 equiv), $Pd(OAc)_2$ (0.05-0.2 equiv), dppf (0.05-0.2 equiv), and *N*,*N*-dimethylacetamide (DMA, 1-2 mL/mmol) was degassed with three vacuum/nitrogen cycles. But-1-yn-1-

yltrimethylsilane (1.3-2.0 equiv) was added, and the reaction was heated at 80 °C under N_2 for 2-24 hours (until complete by TLC or LCMS). The reaction was allowed to cool to room temperature, diluted with ethyl acetate and water, and then filtered through Celite. The aqueous layer was separated and extracted with ethyl acetate. The organics were combined, dried, filtered, concentrated, and then purified by silica gel column chromatography to give the corresponding butynyl-aryl or butynyl-heteroaryl.

5-(But-1-yn-1-yl)-1-(tetrahydro-2H-pyran-2-yl)-1H-indazole (17h)

Step 1: 1-(Tetrahydro-2H-pyran-2-yl)-5-((trimethylsilyl)ethynyl)-1H-indazole (15h):

To a 250-mL pressure tube, 5-bromo-1-(tetrahydro-2H-pyran-2-yl)-1H-indazole (11.9 g, 42.3 mmol), $Pd(Ph_3P)_2Cl_2$ (1.48 g, 0.05 mmol), CuI (0.8 g, 4.2 mmol) and THF/triethylamine (5:1, 85 mL) were added. This mixture was degassed with three vacuum/N_2 cycles, and then trimethylsilylacetylene (9 mL, 63.5 mmol) was added. The pressure tube was sealed and heated at 80 °C for 2 days. Upon completion by LCMS, the reaction mixture was cooled down to room temperature and filtered through Celite with ethyl acetate (200 mL). The filtrate was concentrated to give the crude product that was used directly in the next step.

Step 2: 5-Ethynyl-1-(tetrahydro-2H-pyran-2-yl)-1H-indazole (16h)

A 250-mL round-bottom flask equipped with a magnetic stir bar, a rubber septum, and a N_2 inlet was charged with a solution of 1-(tetrahydro-2H-pyran-2-yl)-5-((trimethylsilyl)ethynyl)-1H-indazole (12.6 g, 42.2 mmol) in MeOH. To this solution, solid K_2CO_3 (0.58 g, 4.2 mmol) was added in one portion. The resulting mixture was stirred at room temperature for 4 h. Upon completion by TLC, the reaction mixture was filtered, concentrated, and purified by silica gel chromatography (0-10% ethyl acetate in hexanes) to give 5-ethynyl-1-(tetrahydro-2H-pyran-2-

yl)-1H-indazole (4.7 g) as a pale yellow solid. ^{1}H NMR (400 MHz, DMSO-d_6): δ 8.13 (s, 1H), 7.96 (s, 1H), 7.75 (d, 1H, J = 8.75 Hz), 7.47 (dd, 1H, J = 1.45 Hz, 8.75 Hz), 5.86 (dd, 1H, J = 2.60 Hz, J = 9.80 Hz), 4.10 (s, 1H), 3.90-3.86 (m, 1H), 3.78-3.68 (m, 1H), 2.43-2.32 (m, 1H), 2.06-1.93 (m, 2H), 1.81-1.66 (m, 1H), 1.60-1.50 (m, 2H).

Step 3: 5-(But-1-yn-1-yl)-1-(tetrahydro-2H-pyran-2-yl)-1H-indazole (17h)

A 250-mL round-bottom flask equipped with a magnetic stir bar, a rubber septum, and a N_2 inlet was charged with 5-ethynyl-1-(tetrahydro-2H-pyran-2-yl)-1H-indazole (4.2 g, 18.6 mmol) and anhydrous THF/TMEDA (9:1, 93 mL). This solution was cooled to -78 °C in an IPA/dry ice bath, and *n*-BuLi (17.4 mL solution in hexanes, 27.84 mmol) was added drop wise over 15 minutes. The resulting mixture was stirred for 30 minutes at -78 °C, and then iodoethane (2.23 mL, 27.84 mmol) was added dropwise over 5 minutes. The mixture was gradually warmed to room temperature, stirred for 1 h, and then heated at 40 °C overnight. Upon completion by LCMS, the reaction mixture was cooled to room temperature, quenched with water (100 mL), and extracted with ethyl acetate (2x100 mL). The combined organics were washed with water (100 mL), washed with brine (50 mL), dried over sodium sulfate, filtered, concentrated, and purified by silica gel chromatography (0-10% ethyl acetate in hexanes) to give 5-(but-1-yn-1-yl)-1-(tetrahydro-2H-pyran-2-yl)-1H-indazole (1.42 g) as a pale yellow solid. ^{1}H NMR (400 MHz, DMSO-d_6): δ 8.08 (s, 1H), 7.82 (s, 1H), 7.68 (d, 1H, J = 8.75 Hz), 7.39 (dd, 1H, J = 1.60 Hz, 8.75 Hz), 5.82 (dd, 1H, J = 2.60 Hz, J = 9.90 Hz), 3.90-3.84 (m, 1H), 3.77-3.69 (m, 1H), 2.43 (q, 2H, J = 7.50 Hz), 2.40-2.33 (m, 1H), 2.04-1.92 (m, 2H), 1.78-1.67 (m, 1H), 1.60-1.53 (m, 2H), 1.18 (t, 3H, J = 7.50 Hz); LCMS: 255 $(M+H)^+$.

Method B: Alternate preparation of 5-(but-1-yn-1-yl)-1-(tetrahydro-2H-pyran-2-yl)-1H-indazole (17h):

A mixture of 5-bromo-1-(tetrahydro-2H-pyran-2-yl)-1H-indazole (39.6 g, 0.142 mol), Cs_2CO_3 (60.0 g, 184 mmol), CuI (1.35 g, 7.08 mmol), $Pd(OAc)_2$ (1.59 g, 7.08 mmol), dppf (3.93 g, 7.08 mmol), and *N,N*-dimethylacetamide (DMA, 160 mL) was degassed with three vacuum/nitrogen cycles. But-1-yn-1-yltrimethylsilane (23.2 g, 184 mmol) was added, and the resulting mixture was heated at 80 °C for 5 h under N_2. Upon completion by LCMS, the reaction mixture was diluted with EtOAc (300 mL) and H_2O (300 mL) and then filtered. The organic layer of the filtrate was separated, and the aqueous layer was extracted with EtOAc (3 x 150 mL). The combined organic layers were washed with brine (2 x 100 mL), dried over anhydrous Na_2SO_4, filtered and concentrated. The residue was purified on silica gel column (300-400 mesh, 20 cm in diameter and 15 cm in height) using EtOAc/petroleum ether (1 L of petroleum ether; then 1 L of EtOAc/petroleum ether = 1/50; and then EtOAc/Petroleum ether = 1/30 until the by-product was washed out; then EtOAc/petroleum ether = 1/10 to collect the product) affording a yellow oil (33 g) which solidified over time in the refrigerator. The resulting solid was further washed with petroleum ether (200 mL, then 3 x 50 mL) affording the title compound as an off-white solid (26 g, 73%). ^{1}H NMR (400 MHz, DMSO-d_6): δ 8.08 (s, 1H), 7.82 (s, 1H), 7.68 (d, 1H, J = 8.75 Hz), 7.39 (dd, 1H, J = 1.60 Hz, 8.75 Hz), 5.82 (dd, 1H, J = 2.60 Hz, J = 9.90 Hz), 3.90-3.84 (m, 1H), 3.77-3.69 (m, 1H), 2.43 (q, 2H, J = 7.50 Hz), 2.40-2.33 (m, 1H), 2.04-1.92 (m, 2H), 1.78-1.67 (m, 1H), 1.60-1.53 (m, 2H), 1.18 (t, 3H, J = 7.50 Hz); ^{13}C NMR (100 MHz, DMDO-d_6): δ 138.2, 133.5, 129.4, 124.0, 123.9, 115.9, 110.7, 90.2, 84.1, 80.1, 66.5, 28.8, 24.7, 22.1, 13.8, 12.3; LCMS: 255 $(M+H)^+$.

Method C: General procedure for multi-component cross-coupling of the butynyl-aryls or butynyl-heteroaryls

A mixture of the appropriate butynyl-aryl or butynyl-heteroaryl (1.0 equiv), aryl-iodide (3.0 equiv), aryl-boronic acid (3.0 equiv), K_2CO_3 (3.0 equiv), and *N*,*N*-dimethylformamide (DMF)/water (2:1, 50 mL/mmol) was degassed with three vacuum/N_2 cycles and then heated at 45 °C. After 10 min (or when homogenous), a solution of $Pd(PhCN)_2Cl_2$ (0.01 equiv) in DMF was added (Note 1). The reaction was stirred at 45 °C for 4-24 h (until complete by TLC or LCMS; Note 2), allowed to cool to room temperature, quenched with water, and then extracted with ethyl acetate. The extracts were washed with water, washed with brine, dried, filtered, concentrated, and purified by silica gel chromatography to give the desired tetra-substituted alkene.

Note 1: In some instances, all chemicals were simply mixed at room temperature, degassed, and then heated. In other instances, the boronic acid was added last as a DMF/water solution. *Note 2:* When incomplete conversion of butynyl-heteroaryl was observed (especially with ortho-substituted aryl-iodides), additional aryl-iodide, aryl-boronic acid, and K_2CO_3 (1-3 equiv each) were added and heating was continued for 8-24 h.

Method D: General procedure for an alternate multi-component cross-coupling of the butynyl-heteraryls

Step 1: Preparation of bis(pinacolato)diboryl-alkene:

A solution of the appropriate butynyl-heteroaryl (1.0 equiv), bis(pinacolato)diboron (1.01 equiv), $Pt(PPh_3)_4$ (0.01 equiv), and 2-methyltetrahydrofuran (2 mL/mmol) was degassed with three vacuum/N_2 cycles and then heated at reflux under N_2 for 1-8 h (until complete by TLC or LCMS). The reaction was allowed to cool to room temperature and then either 1) taken directly

into Step 2; or 2) concentrated to give a crude residue [usually a foam]; or 3) concentrated and purified by silica gel chromatography to afford the pure bis(pinacolato)diboryl-alkene.

Step 2: Cross-coupling of the bis(pinacolato)diboryl-alkene

A mixture of bis(pinacolato)diboryl-alkene (1.0 equiv), an appropriate 4-iodoaryl-aldehyde or (*E*)-ethyl 3-(4-iodophenyl)acrylate (1.0 equiv), $PdCl_2(PPh_3)_2$ (0.1 equiv), Cs_2CO_3 (2 equiv), 2-methyltetrahydrofuran (4 mL/mmol, Note 1), and water (0-3% v/v; Note 2) was stirred vigorously at 20-40 °C (Note 3) under N_2 for 1-24h (until complete by TLC or LCMS). The reaction was then either 1) taken directly into Step 3; or 2) processed to isolate the 1-aryl-2-(pinacolato)boryl-alkene: [The reaction was diluted with ethyl ether (or ethyl acetate) and washed with water (1-3 times). The aqueous phases were back extracted with ethyl ether (or ethyl acetate). The extracts were combined, dried, filtered, concentrated and then purified by silica gel chromatography].

Note 1: When the bis(pinacolato)diboryl-alkene is brought into this step as a solution from Step 1, solvent (2 mL/mmol) is added to make the final volume of solvent approximately 4 mL/mmol. *Note 2:* Most commonly, anhydrous Cs_2CO_3 and anhydrous solvent were used, so 1-2% water (v/v with respect to solvent) was added to the reaction. When the Cs_2CO_3 and/or solvent were not anhydrous, no water was added. *Note 3:* Most commonly, reactions were run at room temperature resulting in higher regio-control.

Step 3: Cross-coupling of the 1-aryl-2-(pinacolato)boryl-alkene

A mixture of 1-aryl-2-(pinacolato)boryl-alkene (1.0 equiv), an appropriate aryl-halide or heteroaryl-halide (1.5 equiv), $PdCl_2(PPh_3)_2$ (0.1 equiv), 2-methyltetrahydrofuran (4 mL/mmol; Note 1), and KOH (3-6M, 5-6 equiv; Note 2) was degassed with three vacuum/N_2 cycles and

then heated at reflux under N_2 for 1-24 h (until complete by TLC or LCMS). The reaction was allowed to cool to room temperature, diluted with ethyl ether (or ethyl acetate), and washed with water (1-3 times). The aqueous phases were back extracted with ethyl ether (or ethyl acetate). The extracts were combined, dried, filtered, concentrated and then purified by silica gel chromatography to give the desired tetra-substituted alkene.

Note 1: When the 1-aryl-2-(pinacolato)boryl-alkene is brought into this step directly from Step 2, no additional solvent or $PdCl_2(PPh_3)_2$ was added. Only the aryl-halide (or heteroaryl-halide) and KOH were added. *Note 2:* Most commonly, 6 equiv of KOH are used, and the aqueous solution of KOH is 4M or 6M. For some compounds, especially those with base-sensitive functionality (e.g. a nitrile or ester), K_2CO_3 (6 equiv, 4M aqueous) is used in place of KOH, and DMSO is used as either the sole solvent or a co-solvent.

Method E: Horner-Wadsworth-Emmons coupling of the aryl-aldehydes

1,8-Diazabicyclo[5.4.0]undec-7-ene (DBU, 1.1 equiv) was added dropwise to a mixture of the appropriate aryl-aldehyde (1.0 equiv), triethylphosphonoacetate (1.1-1.3 equiv), lithium chloride (2.0 equiv), and anhydrous acetonitrile (2 mL/mmol) at room temperature. The resulting mixture was stirred for 1-4 h (until complete by TLC or LCMS) and then concentrated. Dichloromethane (or ethyl acetate or ether) was added, and the mixture was washed with water, washed with brine, dried, filtered, concentrated, and purified by silica gel column chromatography to give the desired acrylic ester.

Method F: Removal of protecting groups

i) Deprotection of a THP group: A solution of HCl (Note 1) was added to a solution of the protected-heteroaryl (1.0 equiv) in ethanol (2-5 mL/mmol; Note 2) at room temperature. The mixture was heated at 70 °C (Note 3) for 2-8 h (until complete by TLC or LCMS), allowed to

cool to room temperature, and concentrated to give a crude product that was either carried on directly to the next step or purified by silica gel chromatography.

Note 1: Most commonly, 2M HCl in diethyl ether or 1.25M HCl in ethanol were used. Most commonly, 10% v/v HCl solution was used. *Note 2:* Most commonly, the concentration was 5 mL/mmol. *Note 3*: In some instances, the reaction was heated at 80 °C or reflux.

ii) Deprotection of a MOM group A variety of conditions have been utilized to remove the MOM protecting group including 1) the same as above for removing THP, 2) ethereal HCl in refluxing THF, 3) aqueous HCl in refluxing ethanol

iii) Deprotection of a Trt or a Boc group: Most commonly, Trt and Boc groups were removed under the conditions described for THP group.

iv) Deprotection of an acetyl group: The N-acetyl group was removed during the hydrolysis of the acrylic ester with LiOH as described in Method G.

Method G: Hydrolysis of the acrylic ester to the acrylic acid

An aqueous solution of LiOH (2-20 equiv; Note 1) was added to a solution of the appropriate ester (1.0 equiv) in ethanol/tetrahydrofuran (1:1, 10 mL/mmol; Note 2) at room temperature, and the mixture was stirred for 4-24 h (until complete by TLC or LCMS). A solution of HCl (1M aqueous) was added until the pH was 3 (Note 3). The mixture was diluted with water and extracted with ethyl acetate. The organic layer was washed with water, washed with brine, dried, filtered, concentrated, and purified by silica gel chromatography or preparative-HPLC to give the desired acrylic acid.

Note 1: Most commonly, a 2M solution of aqueous LiOH was used, or the LiOH was dissolved in minimum amount of water. *Note 2:* In some instances, a single solvent (ethanol, dioxane, or tetrahydrofuran) was used. *Note 3*: Alternate work-up procedures have been employed including:

i) the use of sat'd NH_4Cl in place of aqueous HCl and ii) removal of the organic solvent by rotary evaporation prior to acid quench.

(E)-3-(4-((E)-1-(1H-Indol-5-yl)-2-phenylbut-1-en-1-yl)phenyl)acrylic acid (9e)

The title compound was prepared using 1-(5-(but-1-yn-1-yl)-1H-indol-1-yl)ethanone, (*E*)-(4-(3-ethoxy-3-oxoprop-1-en-1-yl)phenyl)boronic acid and iodobenzene following Methods C and G. ^{1}H NMR (300 MHz, DMSO-d_6): δ OH resonance not observed, 12.30 (br, 1H), 11.13 (s, 1H), 7.43-7.31 (m, 5H), 7.24-7.12 (m, 5H), 6.93-6.88 (m, 1H), 6.87 (d, 2H, J = 8.5 Hz), 6.44-6.40 (m, 1H), 6.36 (d, 1H, J = 16.0 Hz), 2.46 (q, 2H, J = 7.3 Hz), 0.88 (t, 3H, J = 7.3 Hz); HRMS-ESI$^+$: *m/z* $[M+H]^+$ calcd for $C_{27}H_{23}NO_2$, 394.1807; found, 394.1809.

(E)-3-(4-((E)-1-(1H-benzo[d][1,2,3]triazol-5-yl)-2-phenylbut-1-en-1-yl)phenyl)acrylic acid (9g)

The title compound was prepared using 5-(but-1-yn-1-yl)-1-(tetrahydro-2H-pyran-2-yl)-1H-benzo[d][1,2,3]triazole, (*E*)-(4-(3-ethoxy-3-oxoprop-1-en-1-yl)phenyl)boronic acid and iodobenzene following Methods C, F and G. ^{1}H NMR (300 MHz, DMSO-d_6): δ 15.65 (br, 1H), 12.29 (br, 1H), 7.92 (d, 1H, J = 8.40 Hz), 7.78 (s, 1H), 7.41 (d, 1H, J = 16.0 Hz), 7.35 (d, 2H, J = 8.40 Hz), 7.24-7.13 (m, 6H), 6.91 (d, 2H, J = 8.40 Hz), 6.37 (d, 1H, J = 16.0 Hz), 2.39 (q, 2H, J = 7.50 Hz), 0.89 (t, 3H, J = 7.50 Hz).). ^{13}C NMR (100, MHz, DMSO-d_6): δ 167.5, 144.5, 143.3 (2C), 143.2, 143.2, 141.1, 137.3, 131.8, 130.7, 129.3, 128.0, 127.5, 126.6, 118.8, 28.6, 13.2. HRMS-ESI$^+$: *m/z* $[M+H]^+$ calcd for $C_{25}H_{21}N_3O_2$, 396.1712; found, 396.1704.

(E)-3-(4-((E)-1-(1H-indazol-5-yl)-2-phenylbut-1-en-1-yl)phenyl)acrylic acid (9h)

*Step 1: (E)-Ethyl 3-(4-((E)-2-phenyl-1-(1-(tetrahydro-2H-pyran-2-yl)-1H-indazol-5-yl)but-1-en-1-yl)phenyl)acrylate (20h):*A solution of 5-(but-1-yn-1-yl)-1-(tetrahydro-2H-pyran-2-yl)-1H-indazole (2.5 g, 9.83 mmol), iodobenzene (6 g, 29.5 mmol), (*E*)-(4-(3-ethoxy-3-oxoprop-1-en-1-

yl)phenyl)boronic acid (6.49 g, 29.5 mmol), K_2CO_3 (4.08 g, 29.5 mmol), and *N,N*-dimethylformamide/water (2:1, 492 mL) was degassed with 3 vacuum/N_2 cycles and then heated at 45 °C until it was a homogenous solution. A solution of $Pd(PhCN)_2Cl_2$ (38 mg, 0.098 mmol) in *N,N*-dimethylformamide (0.5 mL) was added. The resulting mixture was stirred at 45 °C overnight. Upon completion, the reaction mixture was cooled to room temperature, quenched with water (500 mL), and extracted with ethyl acetate (3x500 mL). The combined organics were washed with water, washed with brine, dried over sodium sulfate, filtered, and concentrated to give the crude product. This crude material was purified on a silica gel column eluted with 0-50% ethyl acetate in hexanes affording the title compound as off-white foam (3.71 g). LCMS: 423 $[(M\text{-}THP+H)+H]^+$.

Step 2: (E)-Ethyl 3-(4-((E)-1-(1H-indazol-5-yl)-2-phenylbut-1-en-1-yl)phenyl)acrylate (21h):

To a solution of (*E*)-ethyl 3-(4-((*E*)-2-phenyl-1-(1-(tetrahydro-2H-pyran-2-yl)-1H-indazol-5-yl)but-1-en-1-yl)phenyl)acrylate (3.5 g, 6.9 mmol) in ethyl alcohol (69 mL), HCl (6mL, 2M in diethyl ether) was added at room temperature. The resulting mixture was then heated at 70 °C for 2 h. Upon completion, the mixture was cooled to room temperature and concentrated to give the crude product. This crude material was purified on a silica gel column eluted with 0-100% ethyl acetate in hexanes affording an off-white solid (2.5 g, 86% yield). ^{1}H NMR (300 MHz, DMSO-d_6): δ 13.10 (s, 1H), 8.08 (s, 1H), 7.69 (s, 1H), 7.53 (d, 1H, J = 8.70 Hz), 7.48 (d, 1H, J = 16.0 Hz), 7.39 (d, 2H, J = 8.40 Hz), 7.27-7.11 (m, 6 H), 6.89 (d, 2H, J = 8.40 Hz), 6.45 (d, 1H, J = 16.0 Hz), 4.14 (q, 2H, J = 7.30 Hz), 2.43 (q, 2H, J = 7.50 Hz), 1.22 (t, 3H, J = 7.30 Hz), 0.87 (t, 3H, J = 7.50 Hz); LCMS: 423 $(M+H)^+$.

Step 3: (E)-3-(4-((E)-1-(1H-Indazol-5-yl)-2-phenylbut-1-en-1-yl)phenyl)acrylic acid (9h)

To a solution of (*E*)-ethyl 3-(4-((*E*)-1-(1H-indazol-5-yl)-2-phenylbut-1-en-1-yl)phenyl)acrylate (2.5 g, 5.9 mmol) in THF-EtOH (1:1, 59 mL), an aqueous solution of LiOH (2.8 g, 118 mmol; dissolved in a minimum amount of water) was added at room temperature. The resulting mixture was stirred at room temperature overnight. The reaction was monitored by LCMS. Upon completion, 1N aqueous HCl was added until pH was 3. Then, the mixture was diluted with water and extracted with ethyl acetate (3x200 mL). The combined organic layers were washed with water, washed with brine, dried over sodium sulfate, filtered, and concentrated to give the crude product. This crude material was purified on a silica gel column eluted with 0-20% methanol in dichloromethane affording the title compound as a pale yellow solid (1.9 g). ^{1}H NMR (400 MHz, DMSO-d_6): δ OH resonance not observed, 12.7 (br, 1H), 8.08 (d, 1H, J = 0.9 Hz), 7.65 (br, 1H), 7.54 (d, 1H, J = 8.50 Hz), 7.44 (d, 1H, J = 16. 0 Hz), 7.33 (d, 2H, J = 8.50 Hz), 7.20-7.08 (m, 6 H), 6.88 (d, 2H, J = 8.40 Hz), 6.37 (d, 1H, J = 16.0 Hz), 2.41 (q, 2H, J = 7.50 Hz), 0.86 (t, 3H, J = 7.50 Hz). ^{13}C NMR (100, MHz, DMSO-d_6): δ 166.4, 144.1, 142.4, 141.4, 140.4, 137.8, 137.0, 133.5, 132.4, 130.4, 129.7, 128.2, 126.8, 126.6, 126.3, 125.3, 121.8, 119.2, 117.4, 108.9, 27.5, 12.2. HRMS-ESI^{+}: *m/z* $[M+H]^{+}$ calcd for $C_{26}H_{22}N_2O_2$, 395.1760; found, 395.1759.

(E)-3-(4-((E)-1-(1H-Indazol-4-yl)-2-phenylbut-1-en-1-yl)phenyl)acrylic acid (9i)

The title compound was prepared using 4-(but-1-yn-1-yl)-1-(tetrahydro-2H-pyran-2-yl)-1H-indazole, (*E*)-(4-(3-ethoxy-3-oxoprop-1-en-1-yl)phenyl)boronic acid and iodobenzene following Methods C, F and G. ^{1}H NMR (400 MHz, DMSO-d_6): δ 13.14 (br s, 1H), 12.31 (br s, 1H), 7.78 (d, 1H, J = 1.0 Hz), 7.49 (d, 1H, J = 8.5 Hz), 7.42-7.37 (m, 2H), 7.33 (d, 2H, J = 8.3 Hz), 7.26-7.22 (m, 4H), 7.20-7.14 (m, 1H), 7.08 (dd, 1H, J = 0.67 Hz, J = 6.9 Hz), 6.95 (d, 2H, J = 8.3 Hz), 6.34 (d, 1H, J = 16.0 Hz), 2.32 (q, 2H), 0.79 (t, 3H). ^{13}C NMR (100 MHz, DMSO-d_6): δ 167.5,

144.2, 143.6, 143.4, 141.0, 140.2, 135.5, 135.0, 132.7, 131.8, 130.2, 129.4, 128.0, 127.5, 126.6, 126.0, 122.4, 120.2, 118.6, 109.1, 28.8, 13.1. HRMS-ESI$^+$: *m/z* $[M+H]^+$ calcd for $C_{26}H_{22}N_2O_2$, 395.1760; found, 395.1760.

(E)-3-(4-((E)-1-(1H-indazol-6-yl)-2-phenylbut-1-en-1-yl)phenyl)acrylic acid (9j)

The title compound was prepared using 6-(but-1-yn-1-yl)-1-(tetrahydro-2H-pyran-2-yl)-1H-indazole, (*E*)-(4-(3-ethoxy-3-oxoprop-1-en-1-yl)phenyl)boronic acid and iodobenzene following Methods C, F and G. ^{1}H NMR (400 MHz, DMSO-d_6): δ 112.94 (br, 1H), 12.40 (br, 1H), 8.07 (d, 1H, *J* = 0.9Hz), 7.75-7.73 (m, 1H), 7.43-7.34 (m, 3H), 7.23-7.12 (m, 5H), 6.94-6.88 (m, 3H), 6.37 (d, 1H, *J* = 16.0 Hz), 2.43 (q, 2H, *J* = 7.50 Hz), 0.88 (t, 3H, *J* = 7.50 Hz). ^{13}C NMR (100 MHz, DMSO-d_6): δ 167.5, 144.7, 143.3, 142.7, 141.3, 140.3, 140.0, 138.0, 133.3, 131.7, 130.7, 129.3, 128.0, 127.4, 126.5, 122.1, 121.6, 120.4, 118.7, 109.9, 28.6, 13.3; HRMS-ESI$^+$: *m/z* $[M+H]^+$ calcd for $C_{26}H_{22}N_2O_2$, 395.1760; found, 395.1752.

(E)-3-(4-((E)-2-(2-chlorophenyl)-1-(1H-indazol-5-yl)but-1-en-1-yl)phenyl)acrylic acid (11a)

The title compound was prepared using 5-(but-1-yn-1-yl)-1-(tetrahydro-2H-pyran-2-yl)-1H-indazole, (*E*)-(4-(3-ethoxy-3-oxoprop-1-en-1-yl)phenyl)boronic acid, and 1-chloro-2-iodobenzene following Methods C, F and G. ^{1}H NMR (400 MHz, DMSO-d_6): δ 8.32 (br, 2H), 8.12 (s, 1H), 7.74 (s, 1H), 7.61 (d, 1H, *J* = 16.0 Hz), 7.53 (d, 1H, *J* = 7.50 Hz), 7.33-7.27 (m, 2H), 7.22-7.20 (m, 2H), 7.17-7.11 (m, 3H), 7.01 (d, 2H, *J* = 8.50 Hz), 6.32 (d, 1H, *J* = 16.0 Hz), 2.48 (q, 2H, *J* = 7.50 Hz), 0.98 (t, 3H, *J* = 7.50 Hz). ^{13}C NMR (100 MHz, DMSO-d_6): δ 171.3, 146.2, 145.2, 140.9, 140.4, 139.8, 138.9, 135.1, 134.3, 133.3., 131.9, 131.7, 130.2, 129.5, 129.3, 128.0, 127.4, 126.3, 123.2, 121.2, 117.0, 109.9, 28.3, 12.9. HRMS-ESI$^+$: *m/z* $[M+H]^+$ calcd for $C_{26}H_{21}ClN_2O_2$, 429.1370; found, 429.1370.

(E)-3-(4-((E)-2-(2-cyanophenyl)-1-(1H-indazol-5-yl)but-1-en-1-yl)phenyl)acrylic acid (11d)

The title compound was prepared using 5-(but-1-yn-1-yl)-1-(tetrahydro-2H-pyran-2-yl)-1H-indazole, (*E*)-(4-(3-ethoxy-3-oxoprop-1-en-1-yl)phenyl)boronic acid, and 2-iodobenzonitrile following Methods C, F and G. ^{1}H NMR (300 MHz, DMSO-d_6): δ OH resonance not observed, 13.17 (s, 1H), 8.13 (br, 1H), 7.68-7.63 (m, 4H), 7.59 (d, 1H, *J* = 8.50 Hz), 7.43-7.36 (m, 4H), 7.19 (dd, 1H, *J* = 1.5 Hz, *J* = 8.50 Hz), 6.92 (d, 2H, *J* = 8.50 Hz), 6.38 (d, 1H, *J* = 16.0 Hz), 2.47 (q, 2H, J = 7.50 Hz), 0.93 (t, 3H, J = 7.50 Hz); HRMS-ESI^{+}: *m/z* $[M+H]^{+}$ calcd for $C_{27}H_{21}N_3O_2$, 420.1712; found, 420.1712.

(E)-3-(4-((E)-1-(1H-indazol-5-yl)-2-(o-tolyl)but-1-en-1-yl)phenyl)acrylic acid (11g)

The title compound was prepared using 5-(but-1-yn-1-yl)-1-(tetrahydro-2H-pyran-2-yl)-1H-indazole, (*E*)-(4-(3-ethoxy-3-oxoprop-1-en-1-yl)phenyl)boronic acid, and 1-iodo-2-methylbenzene following Methods C, F and G. ^{1}H NMR (400 MHz, DMSO-d_6): δ 13.17 (s, 1H), 12.39 (br s, 1H), 8.09 (dd, 1H, *J* = 1.0 Hz), 7.68 (s, 1H), 7.54 (d, 1H, *J* = 8.5 Hz), 7.38 (d, 1H, *J* = 15.9 Hz), 7.31 (d, 2H, *J* = 8.3 Hz), 7.23 (m, 1H), 7.18 (dd, 1H, *J* = 1.5 Hz, *J* = 8.6 Hz), 7.14 (dt, 1H, *J* = 1.5 Hz, *J* = 7.3 Hz), 7.08 (dt, 1H, *J* = 1.5 Hz, *J* = 7.5 Hz), 7.05-7.03 (m, 1H), 6.87 (d, 2H, *J* = 8.3 Hz), 6.34 (d, 1H, *J* = 16.0 Hz), 2.38-2.29 (m, 2H), 2.12 (s, 3H), 0.87 (t, 3H, J = 7.50 Hz); ^{13}C NMR (100 MHz, DMSO-d_6): δ 167.5, 144.8, 143.4, 141.0, 140.6, 138.9, 138.5, 135.0, 134.3, 133.6, 131.7, 129.9, 129.5, 127.8, 127.2, 126.6, 125.3, 122.9, 120.4, 118.6, 110.1, 29.3, 19.4, 12.4. HRMS-ESI^{+}: *m/z* $[M+H]^{+}$ calcd for $C_{27}H_{24}N_2O_2$, 409.1916; found, 409.1916.

(E)-3-(4-((E)-1-(1H-indazol-5-yl)-2-(2-(methylsulfonyl)phenyl)but-1-en-1-yl)phenyl)acrylic acid (11h)

Step 1: (E)-Ethyl 3-(4-((E)-2-(2-(methylthio)phenyl)-1-(1-(tetrahydro-2H-pyran-2-yl)-1H-indazol-5-yl)but-1-en-1-yl)phenyl)acrylate

The title compound was prepared using 5-(but-1-yn-1-yl)-1-(tetrahydro-2H-pyran-2-yl)-1H-indazole, (*E*)-(4-(3-ethoxy-3-oxoprop-1-en-1-yl)phenyl)boronic acid, and 2-iodothioanisole following Method C. ^{1}H NMR (300MHz, DMSO-d_6): δ 8.14 (s, 1H), 7.75 (d, 1H, *J* =8.50 Hz), 7.72-7.65 (m, 1H), 7.44 (d, 1H, *J* = 16.0 Hz), 7.35 (d, 2H, *J* = 8.50 Hz), 7.29-7.24 (m, 1H), 7.22-7.11 (m, 3H), 7.09-7.03 (m, 1H), 7.01 (d, 2H, *J* = 8.30 Hz), 6.44 (d, 1H, *J* = 16.0 Hz), 5.85 (dd, 1H, *J* = 2.50 Hz, *J* = 10.0 Hz), 4.13 (q, 2H, *J* = 7.20 Hz), 3.94-3.83 (m, 1H), 3.80-3.68 (m, 1H), 2.47-2.27 (m, 6H), 2.09-1.93 (m, 2H), 1.83-1.69 (m, 1H), 1.67-1.52 (m, 2H), 1.20 (t, 3H, *J* = 7.20 Hz), 0.88 (t, 3H, *J* = 7.60 Hz).

Step 2: (E)-Ethyl 3-(4-((E)-2-(2-(methylsulfonyl)phenyl)-1-(1-(tetrahydro-2H-pyran-2-yl)-1H-indazol-5-yl)but-1-en-1-yl)phenyl)acrylate (26h)

Oxone (potassium peroxymonosulfate; 521 mg, 0.85 mmol) was added to a slurry of (*E*)-ethyl 3-(4-((*E*)-2-(2-(methylthio)phenyl)-1-(1-(tetrahydro-2H-pyran-2-yl)-1H-indazol-5-yl)but-1-en-1-yl)phenyl)acrylate (156 mg, 0.28 mmol) in MeOH:H_2O (1:1, 6 mL) at room temperature, and the reaction was stirred overnight. Dichloromethane and water were added, and the layers were separated. The aqueous layer was washed with dichloromethane (x 2). The organic layers were combined, washed with water, washed with brine, dried over Na_2SO_4, filtered, and concentrated. The crude material was purified on a silica gel column eluted with 0-50% ethyl acetate in hexane affording the title compound. ^{1}H NMR (300MHz, DMSO-d_6): δ 8.15 (s, 1H), 7.91 (d, 1H, *J* = 8.0 Hz), 7.77-7.71 (m, 2H), 7.49-7.46 (m, 3H), 7.41-7.31 (m, 4H), 7.01 (d, 2H, *J* = 8.20 Hz), 6.45 (d, 1H, *J* =16.0 Hz), 5.87 (dd, 1H, *J* = 2.50 Hz, *J* = 10.0 Hz), 4.12 (q, 2H, *J* = 7.20 Hz), 3.92-3.85 (m, 1H), 3.82-3.69 (m, 1H), 2.93 (s, 3H), 2.46-2.27 (m, 2H), 2.09-1.97 (m, 3H), 1.85-1.67 (m,

1H), 1.63-1.51 (m, 2H), 1.18 (t, 3H, *J* =7.20 Hz), 0.83 (t, 3H, *J* = 7.60 Hz). LCMS: 501 [(M-THP+H)+H]$^+$.

Step 3: (E)-3-(4-((E)-1-(1H-indazol-5-yl)-2-(2-(methylsulfonyl)phenyl)but-1-en-1-yl)phenyl)acrylic acid (11h)

The title compound was prepared from (*E*)-ethyl 3-(4-((*E*)-2-(2-(methylsulfonyl)phenyl)-1-(1-(tetrahydro-2H-pyran-2-yl)-1H-indazol-5-yl)but-1-en-1-yl)phenyl)acrylate following Methods F and G. ^{1}H NMR (300MHz, DMSO-d_6): δ 13.14 (br s, 1H), 12.29 (br s, 1H), 8.11 (d, 1H, *J* = 0.9 Hz), 7.92 (dd, 1H, *J* = 0.9 Hz, 8.5 Hz), 7.71 (s, 1H), 7.66-7.54 (m, 2H), 7.51-7.44 (m, 2H), 7.40-7.33 (m, 3H), 7.26 (dd, 1H, *J* = 1.50 Hz, *J* = 8.45 Hz), 7.01 (d, 2H, *J* = 8.45 Hz), 6.34 (d, 1H, *J* = 16. 0 Hz), 2.94 (s, 3H), 2.42-2.30 (m, 2H), 0.83 (t, 3H, *J* = 7.60 Hz); HRMS-ESI$^+$: *m/z* [M+H]$^+$ calcd for $C_{27}H_{24}N_2O_4S$, 473.1535; found, 473.1535.

(E)-3-(4-((E)-1-(1H-indazol-5-yl)-2-(2-methoxyphenyl)but-1-en-1-yl)phenyl)acrylic acid (11i)

The title compound was prepared using 5-(but-1-yn-1-yl)-1-(tetrahydro-2H-pyran-2-yl)-1H-indazole, (*E*)-(4-(3-ethoxy-3-oxoprop-1-en-1-yl)phenyl)boronic acid, and 1-iodo-2-methoxybenzene following Methods C, F and G. ^{1}H NMR (400 MHz, DMSO-d_6): δ 13.06 (s, 1H), 12.32 (br, 1H), 8.08 (d, 1H, *J* = 0.9 Hz), 7.65 (s, 1H), 7.53 (d, 1H, *J* = 8.50 Hz), 7.39 (d, 1H, *J* = 16.0 Hz), 7.32 (d, 2H, *J* = 8.50 Hz), 7.18-7.12 (m, 2H), 6.96-6.89 (m, 4H), 6.75 (dt, 1H, *J* = 0.9 Hz, *J* = 7.40 Hz), 6.34 (d, 1H, *J* = 16. 0 Hz), 3.76 (s, 3H), 2.42-2.29 (m, 2H), 0.87 (t, 3H, *J* = 7.50 Hz); ^{13}C NMR (100 MHz, DMSO-d_6): δ 167.5, 156.8, 145.4, 143.5, 139.9, 138.8, 138.6, 134.0, 133.6, 131.6, 131.0, 130.3, 129.7, 128.0, 127.9, 127.3, 122.8, 120.4, 120.0, 118.4, 110.9, 109.9, 55.3, 27.3, 13.1. HRMS-ESI$^+$: *m/z* [M+H]$^+$ calcd for $C_{27}H_{24}N_2O_3$, 425.1865; found, 425.1862.

(E)-Ethyl 3-(4-((Z)-1-(1-(tetrahydro-2H-pyran-2-yl)-1H-indazol-5-yl)-2-(4,4,5,5-tetramethyl-1,3,2-dioxaborolan-2-yl)but-1-en-1-yl)phenyl)acrylate

Step 1: (Z)-5-(1,2-bis(4,4,5,5-tetramethyl-1,3,2-dioxaborolan-2-yl)but-1-en-1-yl)-1-(tetrahydro-2H-pyran-2-yl)-1H-indazole (28)

The title compound was prepared from of 5-(but-1-yn-1-yl)-1-(tetrahydro-2H-pyran-2-yl)-1H-indazole, bis(pinacolato)diboron, and $Pt(PPh_3)_4$ following Method D, Step 1. ^{1}H NMR (400 MHz, DMSO-d_6): δ 8.06 (br, 1H), 7.66 (d, 1H, J = 8.70 Hz), 7.33 (br, 1H), 7.05 (dd, 1H, J = 1.60 Hz, J = 8.70 Hz), 5.81 (dd, 1H, J = 2.50 Hz, J = 9.80 Hz), 3.89 (d, 1H, J = 11.0 Hz), 3.76-3.70 (m, 1H), 2.46-2.36 (m, 1H), 2.0-1.94 (m, 4H), 1.77-1.68 (m, 1H), 1.61-1.54 (m, 2H), 1.27 (s, 12H), 1.16 (s, 12H), 0.87 (t, 3H, J = 7.60 Hz).

Step 2: (E)-Ethyl 3-(4-((Z)-1-(1-(tetrahydro-2H-pyran-2-yl)-1H-indazol-5-yl)-2-(4,4,5,5-tetramethyl-1,3,2-dioxaborolan-2-yl)but-1-en-1-yl)phenyl)acrylate

The title compound was prepared from (*Z*)-5-(1,2-bis(4,4,5,5-tetramethyl-1,3,2-dioxaborolan-2-yl)but-1-en-1-yl)-1-(tetrahydro-2H-pyran-2-yl)-1H-indazole and (*E*)-ethyl 3-(4-iodophenyl)acrylate following Method D, Step 2. ^{1}H NMR (400 MHz, DMSO-d_6): δ 8.09 (s, 1H), 7.70 (d, 1H, J = 8.80 Hz), 7.58-7.63 (m, 3H), 7.49 (s, 1H), 7.11 (d, 2H, J = 8.40 Hz), 6.58 (d, 1H, J = 16.0 Hz), 5.84 (dd, 1H, J = 2.60, J = 9.90 Hz), 4.18 (q, 2H, J = 7.20 Hz), 3.86-3.91 (m, 1H), 3.70-3.77 (m, 1H), 2.36-2.48 (m, 1H), 2.08-2.15 (m, 2H), 1.95-2.08 (m, 2H), 1.70-1.81 (m, 1H), 1.56-1.62 (m, 2H), 1.25 (t, 3H, J = 7.20 Hz), 1.12 (s, 12H), 1.01 (t, 3H, J = 7.50 Hz); LCMS: 473 $[(M\text{-}THP+H)+H]^+$.

(E)-3-(4-((E)-2-(2-chloro-4-fluorophenyl)-1-(1H-indazol-5-yl)but-1-en-1-yl)phenyl)acrylic acid (11l)

Steps 1: (E)-4-(2-(2-chloro-4-fluorophenyl)-1-(1-(tetrahydro-2H-pyran-2-yl)-1H-indazol-5-yl)but-1-en-1-yl)benzaldehyde (33l)

A round-bottom flask equipped with a magnetic stir bar, a reflux condenser, an internal thermometer, and a N_2 inlet was charged with 5-(but-1-yn-1-yl)-1-(tetrahydro-2H-pyran-2-yl)-1H-indazole (50.0 g, 197 mmol), bis(pinacolato)diboron (50.4 g, 199 mmol), and anhydrous 2-methyltetrahydrofuran (393 mL) followed by $Pt(PPh_3)_4$ (1.83 g, 1.5 mmol). This mixture was degassed with three vacuum/N_2 cycles, heated at 83 °C (internal temperature; oil bath at 95 °C) for 5 h under N_2, and then allowed to cool to room temperature. 2-Methyltetrahydrofuran (393 mL), cesium carbonate (128.1 g, 393 mmol), and water (11.8 mL, 1.5% v/v) were added, and the reaction was cooled to 4 °C. 4-Iodobenzaldehyde (45.6 g, 197 mmol) and $PdCl_2(PPh_3)_2$ (6.90 g, 9.8 mmol) were added, and the reaction was degassed with three vacuum/N_2 cycles. The mixture was allowed to warm to room temperature and stirred overnight. Aqueous KOH solution (4M, 275 mL, 1100 mmol) and 2-chloro-4-fluoroiodobenzene (70.6 g, 275 mmol) were added. The reaction was degassed with three vacuum/N_2 cycles, heated at 75 °C (internal temperature; oil bath at 90 °C) for 7 h under N_2, and then allowed to cool to room temperature. The layers were separated, and the organic layer was washed with brine (800 mL), dried over sodium sulfate, filtered, and concentrated. The crude product was purified by silica gel chromatography (0-20% ethyl acetate in hexanes) to give the title compound (82.6 g, 7:1 mixture of regioisomers) as a pale yellow foam. Data for major isomer: (*E*)-4-(2-(2-chloro-4-fluorophenyl)-1-(1-(tetrahydro-2H-pyran-2-yl)-1H-indazol-5-yl)but-1-en-1-yl)benzaldehyde: ^{1}H NMR (300 MHz, DMSO-d_6): δ 9.82 (s, 1H), 8.15 (s, 1H), 7.78-7.71 (m, 2H), 7.61 (d, 2H, J = 8.40 Hz), 7.43-7.27 (m, 3H), 7.15 (m, 3H), 5.86 (dd, 1H, J = 2.40 Hz, J = 9.90 Hz), 3.93-3.85 (m, 1H), 3.79-3.68 (m, 1H),

2.44-2.36 (m, 3H), 2.10-1.96 (m, 2H), 1.81-1.67 (m, 1H), 1.63-1.53 (m, 2H), 0.92 (t, 3H, *J* = 7.20 Hz); LCMS: 405 $[(M\text{-}THP+H)+H]^+$.

Step 2: (E)-Ethyl 3-(4-((E)-2-(2-chloro-4-fluorophenyl)-1-(1-(tetrahydro-2H-pyran-2-yl)-1H-indazol-5-yl)but-1-en-1-yl)phenyl)acrylate (34l)

A round-bottom flask equipped with a magnetic stir bar, an addition funnel, and a N_2 inlet was charged with (*E*)-4-(2-(2-chloro-4-fluorophenyl)-1-(1-(tetrahydro-2H-pyran-2-yl)-1H-indazol-5-yl)but-1-en-1-yl)benzaldehyde (82.6 g, 169 mmol), triethylphosphonoacetate (40.6 mL, 203 mmol), lithium chloride (14.5 g, 338 mmol), and anhydrous acetonitrile (338 mL). The reaction was cooled to 0 °C and then degassed with three vacuum/N_2 cycles. A solution of DBU (27.8 mL, 186 mmol) in acetonitrile (60 mL) was added dropwise over 35 min, and then the ice water bath was removed. The reaction was stirred at room temperature for 1 h, concentrated, and then partitioned between dichloromethane (250 mL) and H_2O (250 mL). The layers were separated, and the organic layer was washed with brine (400 mL), dried over sodium sulfate, filtered, and concentrated. The crude product was purified on a silica gel column (300 g column, 20% ethyl acetate in hexanes) to give the title compound (89.6 g) as a pale yellow foam. ^{1}H NMR (300 MHz, DMSO-d_6): δ 8.14 (s, 1H), 7.75 (d, 1H, *J* = 8.70 Hz), 7.70-7.69 (m, 1H), 7.47 (d, 1H, *J* = 16.0 Hz), 7.42 (d, 2H, *J* = 8.40 Hz), 7.37-7.33 (m, 2H), 7.29 (m, 1H), 7.14 (dt, 1H, *J* = 2.60 Hz, *J* =8.50 Hz), 6.95 (d, 2H, *J* = 8.40 Hz), 6.48 (d, 1H, *J* = 16.0 Hz), 5.86 (dd, 1H, *J* = 2.42 Hz, *J* = 9.80 Hz), 4.14 (q, 2H, *J* = 7.20 Hz), 3.90-3.86 (m, 1H), 3.78-3.70 (m, 1H), 2.45-2.34 (m, 1H), 2.37 (q, 2H, *J* = 7.50 Hz), 2.06-1.95 (m, 2H), 1.78-1.67 (m, 1H), 1.62-1.53 (m, 2H), 1.19 (t, 3H, *J* = 7.20 Hz), 0.90 (t, 3H, *J* = 7.50 Hz); LCMS: 475 $[(M\text{-}THP+H)+H]^+$.

Step 3: (E)-Ethyl 3-(4-((E)-2-(2-chloro-4-fluorophenyl)-1-(1H-indazol-5-yl)but-1-en-1-yl)phenyl)acrylate hydrochloride

A round-bottom flask equipped with a magnetic stir bar was charged with (*E*)-ethyl 3-(4-((*E*)-2-(2-chloro-4-fluorophenyl)-1-(1-(tetrahydro-2H-pyran-2-yl)-1H-indazol-5-yl)but-1-en-1-yl)phenyl)acrylate (255.9 g, 457.8 mmol) and a solution of HCl (732 mL, 1.25 M in ethyl alcohol). The reaction was heated at 80 °C for 2.5 h, allowed to cool to room temperature, and then concentrated to an orange gel. *tert*-Butyl methyl ether (2.3 L) was added. After stirring for 5 min, solids began to precipitate. The mixture was stirred at room temperature for 2 h and then filtered. The solids were washed with MTBE (700 mL) and dried to give the title compound (193 g) as an off-white solid. ^{1}H NMR (400 MHz, DMSO-d_6): δ NH resonance not observed, 8.11 (d, 1H, J = 0.9 Hz), 7.69 (br, 1H), 7.56 (d, 1H, J = 8.60 Hz), 7.46 (d, 1H, J = 16.0 Hz), 7.41 (d, 2H, J = 8.40 Hz), 7.35-7.33 (m, 2H), 7.19 (dd, 1H, J = 1.60 Hz, J = 8.40 Hz), 7.12 (dt, 1H, J = 2.60 Hz, J = 8.60 Hz), 6.96 (d, 2H, J = 8.40 Hz), 6.48 (d, 1H, J = 16.0 Hz), 4.14 (q, 2H, J = 7.20 Hz), 2.38 (q, 2H, J = 7.60 Hz), 1.19 (t, 3H, J = 7.20 Hz), 0.90 (t, 3H, J = 7.50 Hz); LCMS: 475 $(M+H)^+$.

*Step 4: (E)-3-(4-((E)-2-(2-chloro-4-fluorophenyl)-1-(1H-indazol-5-yl)but-1-en-1-yl)phenyl)acrylic acid (**11l**)*

A round-bottom flask equipped with a magnetic stir bar was charged with (*E*)-ethyl 3-(4-((*E*)-2-(2-chloro-4-fluorophenyl)-1-(1H-indazol-5-yl)but-1-en-1-yl)phenyl)acrylate hydrochloride (198.5 g, 388 mmol) and ethyl alcohol (517 mL). A solution of LiOH (27.9 g, 1164 mmol) in water (388 mL) was added, and the mixture was stirred at room temperature overnight. The ethyl alcohol was removed by rotary evaporation, and the remaining solution was cooled to 0 °C and acidified with 2M aqueous HCl to pH 3. Dichloromethane (500 mL) was added, the mixture was stirred, and then the layers were separated. The organic layer was washed with water, washed with brine, dried over sodium sulfate, filtered, and concentrated. The crude product was purified

on a silica column (800 g column, 5% MeOH in DCM) to give the title compound. The product was then dissolved in DCM (400 mL), and acetonitrile (500 mL) was added. Approximately 200 mL of DCM was removed by rotary evaporation (solids began to precipitate). Acetonitrile (550 mL) was added followed by water (25 mL). The mixture was stirred at room temperature for 2 h. The solvent was decanted, and then acetonitrile: DCM (10:1; 550 mL) was added. The mixture stirred at room temperature for 1.5 h, the solvent was again decanted, and then acetonitrile: DCM (10:1; 550 mL) was added. The mixture was again stirred at room temperature for 1.5 h and then filtered. The solids were re-suspended in acetonitrile: DCM (10:1; 550 mL), stirred at room temperature for 1.5h, filtered, and washed to give the title compound (123.9 g) as an off-white powder. ^{1}H NMR (400 MHz, DMSO-d_6): δ 13.11 (br s, 1H), 12.32 (br, 1H), 8.10 (d, 1H, J = 1.0 Hz), 7.68 (s, 1H), 7.55 (d, 1H, J = 8.6 Hz), 7.42-7.33 (m, 5H), 7.18 (dd, 1H, J = 1.5 Hz, J = 8.6 Hz), 7.13 (dt, 1H, J = 2.8 Hz, J = 8.4 Hz), 6.95 (d, 2H, J = 8.4 Hz), 6.37 (d, 1H, J = 16.0 Hz), 2.37 (q, 2H, J = 7.50 Hz), 0.90 (t, 3H, J = 7.50 Hz). ^{13}C NMR (100 MHz, DMSO-d_6): δ 167.5, 160.7 (1C, J = 245 Hz), 144.4, 143.3, 140.7, 139.0, 138.2, 136.4 (1C, J = 3 Hz), 133.6, 133.5, 133.2 (1C, J = 9 Hz), 133.1 (1C, J = 11 Hz), 132.1, 129.6, 127.5, 127.4, 122.8, 120.3, 118.9, 116.13 (1C, J = 25 Hz), 114.0 (1C, J = 21 Hz), 110.18, 27.9, 12.5. HRMS-ESI^{+}: $[M+H]^{+}$ calcd for $C_{26}H_{20}ClFN_2O_2$, 447.1276; found, 447.1276.

Experimental Protocols (Biology)

Breast Cancer Cell ER-α In Cell Western Assay (ER-α degradation assay)

MCF-7 cells were trypsinized and washed twice in phenol red free RPMI containing 5% charcoal dextran stripped FBS with 20 mM HEPES and NEAA and adjusted to a concentration of 200,000

cells per mL with the same medium. Next, 16 μL of the cell suspension (3200 cells) was added to each well of a poly-D-lysine coated 384 well plate, and the cells were incubated at 37 °C over 4 days to allow the cells to adhere and grow. On day 4, a ten point, serial 1:5 dilution of each compound was added to the cells in 16 μL at a final concentration ranging from 10-5M to 5.12 x 10-12M or 10-6M to 5.12 x 10-13M for fulvestrant. At 4 hours post compound addition, the cells were fixed by adding 16 μL of 30% formalin to the 32 μL of cells and compound (10% formalin final concentration) for 20 minutes. Cells were then washed twice with PBS Tween 0.1% and then permeabilized in PBS 0.1% Triton (50μl/well) for additional 15 minutes. The PBS 0.1% triton was decanted, and the cells were washed: LI-COR blocking buffer (50 μL/well) was added, the plate was spun at 3000 rpm, and then the blocking buffer was decanted. Additional LI-COR blocking buffer (50 μL/well) was added, and the cells were incubated overnight at 4 °C. The blocking buffer was decanted, and the cells were incubated overnight at 4 °C with SP1 (Thermo Scientific) anti-ER rabbit monoclonal antibody diluted 1:1000 in LI-COR blocking buffer/0.1% Tween-20. Wells which were treated with blocking buffer with Tween but no antibody were used as a background control. Wells were washed twice with PBS Tween 0.1% to remove free SP1 antibodies, and the cells were incubated at room temp for 60-90 minutes in LI-COR goat anti-rabbit IRDyeTM 800CW (1:1000) and DRAQ5 DNA dye (1:10000 of 5 mM stock solution) diluted in LI-COR blocking buffer containing 0.1% Tween-20 and 0.01% SDS. Cells were then washed with 0.1%Tween-20/PBS three times. Plates were scanned on a LI-COR Odyssey infrared imaging system. Integrated intensities in the 800 nm channel and 700 nm channel were measured to determine levels of ER-α and DNA respectively. Percent ER levels were determined as follows: (Integrated intensity 800 nm sample/integrated intensity 700 nm

sample)/ (Integrated intensity 800 nm untreated cells/integrated intensity 700 nm untreated cells) x 100 = %ER-α levels.

Breast Cancer Cell Viability Assay (MCF-7 viability assay)

MCF-7 cells were adjusted to a concentration of 40,000 cells per mL in RPMI containing 10% FBS and 20 mM HEPES. 16 microliters of the cell suspension (640 cells) was added to each well of a 384 well plate, and the cells were incubated overnight to allow the cells to adhere. The following day a 10 point, serial 1:5 dilution of each compound was added to the cells in 16 µL at a final concentration ranging from 10-0.000005 µM. After 5 days' compound exposure, 16 µL of CellTiter-GLo (Promega) was added to the cells, and the relative luminescence units (RLUs) of each well were determined. CellTiter-Glo added to 32 µL of medium without cells was used to obtain a background value. The percent viability of each sample was determined as follows: (RLU sample-RLU background/RLU untreated cells-RLU background) x 100 = %viability.

Immature Uterine Wet Weight-Antagonist Mode

Female immature CD-IGS rats (21 days old upon arrival) were dosed daily for three days. Vehicle or test compound was administered orally by gavage followed 15 minutes later by an oral dose of 0.1 mg/kg Ethynyl Estradiol. On the fourth day 24 hours after dose, plasma was collected for pharmacokinetic analysis. Immediately following plasma collection, the animals were euthanized and the uterus was removed and weighed.

In-vivo Xenograft Breast Cancer Model; (MCF-7; Tamoxifen-sensitive)

Time release pellets containing 0.72 mg 17-β Estradiol were subcutaneously implanted into nu/nu mice. MCF-7 cells were grown in RPMI containing 10% FBS at 5% CO_2, 37 °C.

Trypsinized cells were pelleted and re-suspended in 50% RPMI (serum free) and 50% Matrigel at $1X10^7$ cells/mL. MCF-7 cells were subcutaneously injected (100µL/animal) on the right flank 2-3 days post pellet implantation. Tumor volume (length x width^2/2) was monitored bi-weekly. When tumors reached an average volume of ~200 mm^3 animals were randomized and treatment was started. Animals were treated with vehicle or compound daily for 4 weeks. Tumor volume and body weight were monitored bi-weekly throughout the study.

In-vivo Xenograft Breast Cancer Model; (Tamoxifen-resistant model)

Female nu/nu mice (with supplemental 17-β Estradiol pellets; 0.72mg; 60 day slow release) bearing MCF-7 tumors (mean tumor volume 200mm^3) were treated with Tamoxifen (citrate) by oral gavage. Tumor volume (length x width^2/2) and body weight were monitored twice weekly. Following a significant anti-tumor response in which tumor volume remained static, evident tumor growth was first observed at approximately 100 days of treatment. At 120 days of treatment, tamoxifen dose was increased. Rapidly growing tumors were deemed tamoxifen resistant and selected for in vivo passage into new host animals. Tumor Fragments (~100mm^3/animal) from the tamoxifen resistant tumors were subcutaneously implanted into the right flank of female nu/nu mice (with 17-β Estradiol pellets (0.72mg; 60 day slow release)). Passaged tumors were maintained under constant Tamoxifen selection, and tumor volume (length x width^2/2) was monitored weekly. When tumor volume reached ~150-250 mm^3, animals were randomized into treatment groups (mean tumor volume 200 mm^3) and tamoxifen treatment was terminated. Animals were treated with vehicle or compound daily for 4 weeks. Tumor volume and body weight were monitored twice weekly for the duration of the study.

AUTHOR INFORMATION

Corresponding author:

*Phone: 858-369-7604. E-mail: nsmith@seragonpharm.com.

Notes: The authors declare no competing financial interest

ABBREVIATIONS

AUC, area under the curve; Cl, clearance; C_{24}, concentration at 24 hours; Cpd, compound; C_{max}, maximum concentration; C_{min}, minimum concentration; CYP, cytochrome; DBU, diazabicycloundecene; DHP, 3,4-dihydro-2H-pyran; dppf, 1,1'-bis(diphenylphosphino)ferrocene; DMAP, 4-dimethylaminopyridine; E2, estradiol; EE, ethynyl estradiol; ER, estrogen receptor; ERE, estrogen response element; FES-PET, 18F-fluoroestradiol positron emission tomography; MOM-Cl, chloro(methoxy)methane; %F, iv; intra-venous, percent oral bioavailability; PG, protecting group; po, per oral; PPTS, pyridinium p-toluenesulfonate; SAR, structure activity relationship; SERD, selective estrogen receptor degrader; SERM, selective estrogen receptor modulator; $t_{1/2}$, half-life; TEA, triethylamine; THP, tetrahydropyran; Tr, triphenylmethane; UWW, uterine wet weight; Vss, volume of distribution at steady state.

REFERENCES

1. Nilsson, S.; Gustafsson, J. A., Estrogen receptors: therapies targeted to receptor subtypes. *Clinical pharmacology and therapeutics* **2011,** *89* (1), 44-55.

2. Ariazi, E. A.; Ariazi, J. L.; Cordera, F.; Jordan, V. C., Estrogen receptors as therapeutic targets in breast cancer. *Current topics in medicinal chemistry* **2006,** *6* (3), 181-202.

3. Riggins, R. B.; Schrecengost, R. S.; Guerrero, M. S.; Bouton, A. H., Pathways to tamoxifen resistance. *Cancer letters* **2007,** *256* (1), 1-24.

4. Musgrove, E. A.; Sutherland, R. L., Biological determinants of endocrine resistance in breast cancer. *Nature reviews. Cancer* **2009,** *9* (9), 631-643.

5. (a) Li, S.; Shen, D.; Shao, J.; Crowder, R.; Liu, W.; Prat, A.; He, X.; Liu, S.; Hoog, J.; Lu, C.; Ding, L.; Griffith, Obi L.; Miller, C.; Larson, D.; Fulton, Robert S.; Harrison, M.; Mooney, T.; McMichael, Joshua F.; Luo, J.; Tao, Y.; Goncalves, R.; Schlosberg, C.; Hiken, Jeffrey F.; Saied, L.; Sanchez, C.; Giuntoli, T.; Bumb, C.; Cooper, C.; Kitchens, Robert T.; Lin, A.; Phommaly, C.; Davies, Sherri R.; Zhang, J.; Kavuri, Megha S.; McEachern, D.; Dong, Yi Y.; Ma, C.; Pluard, T.; Naughton, M.; Bose, R.; Suresh, R.; McDowell, R.; Michel, L.; Aft, R.; Gillanders, W.; DeSchryver, K.; Wilson, Richard K.; Wang, S.; Mills, Gordon B.; Gonzalez-Angulo, A.; Edwards, John R.; Maher, C.; Perou, Charles M.; Mardis, Elaine R.; Ellis, Matthew J., Endocrine-Therapy-Resistant ESR1 Variants Revealed by Genomic Characterization of Breast-Cancer-Derived Xenografts. *Cell Reports 4* (6), 1116-1130; (b) Robinson, D. R.; Wu, Y.-M.; Vats, P.; Su, F.; Lonigro, R. J.; Cao, X.; Kalyana-Sundaram, S.; Wang, R.; Ning, Y.; Hodges, L.; Gursky, A.; Siddiqui, J.; Tomlins, S. A.; Roychowdhury, S.; Pienta, K. J.; Kim, S. Y.; Roberts, J. S.; Rae, J. M.; Van Poznak, C. H.; Hayes, D. F.; Chugh, R.; Kunju, L. P.; Talpaz, M.; Schott, A. F.; Chinnaiyan, A. M., Activating ESR1 mutations in hormone-resistant metastatic breast cancer. *Nat Genet* **2013,** *45* (12), 1446-1451; (c) Toy, W.; Shen, Y.; Won, H.; Green, B.; Sakr, R. A.; Will, M.; Li, Z.; Gala, K.; Fanning, S.; King, T. A.; Hudis, C.; Chen, D.; Taran, T.; Hortobagyi, G.; Greene, G.; Berger, M.; Baselga, J.; Chandarlapaty, S., ESR1 ligand-binding domain mutations in hormone-resistant breast cancer. *Nat Genet* **2013,** *45* (12), 1439-1445.

6. (a) Johnston, S. J.; Cheung, K. L., Fulvestrant - a novel endocrine therapy for breast cancer. *Curr Med Chem* **2010,** *17* (10), 902-914; (b) Pike, A. C.; Brzozowski, A. M.; Walton, J.; Hubbard, R. E.; Thorsell, A. G.; Li, Y. L.; Gustafsson, J. A.; Carlquist, M., Structural insights into the mode of action of a pure antiestrogen. *Structure* **2001,** *9* (2), 145-153; (c) Gradishar, W. J.; Sahmoud, T., Current and future perspectives on fulvestrant. *Clinical breast cancer* **2005,** *6 Suppl 1*, S23-29.

7. Van Kruchten, M.; de Vries, E.G.; Glaudemans, A.W.; van Lanschot, M.C.; van Faassen, M.; Kema, I.P.; Brown, M.; Schroder, C.P.; de Vries, E.F.; Hospers, G.A., Measuring residual estrogen receptor availability during fulvestrant therapy in patients with metastatic breast cancer. *Cancer Discovery,* **2015**, *5*(1): 72-81.

8. (a) Willson, T. M.; Henke, B. R.; Momtahen, T. M.; Charifson, P. S.; Batchelor, K. W.; Lubahn, D. B.; Moore, L. B.; Oliver, B. B.; Sauls, H. R.; Triantafillou, J. A.; et al., 3-[4-(1,2-Diphenylbut-1-enyl)phenyl]acrylic acid: a non-steroidal estrogen with functional selectivity for bone over uterus in rats. *Journal of medicinal chemistry* **1994,** *37* (11), 1550-1552; (b) Wu, Y. L.; Yang, X.; Ren, Z.; McDonnell, D. P.; Norris, J. D.; Willson, T. M.; Greene, G. L., Structural basis for an unexpected mode of SERM-mediated ER antagonism. *Molecular cell* **2005,** *18* (4), 413-424.

9. Slade, D. J.; Pelz, N. F.; Bodnar, W.; Lampe, J. W.; Watson, P. S., Indazoles: regioselective protection and subsequent amine coupling reactions. *The Journal of organic chemistry* **2009,** *74* (16), 6331-6334.

10. Negishi, E.; Anastasia, L., Palladium-catalyzed alkynylation. *Chemical reviews* **2003,** *103* (5), 1979-2017.

11. Zhou, C.; Larock, R. C., Regio- and stereoselective route to tetrasubstituted olefins by the palladium-catalyzed three-component coupling of aryl iodides, internal alkynes, and arylboronic acids. *The Journal of organic chemistry* **2005,** *70* (10), 3765-3777.

12. Tatsuo, I.; Nobuo, M.; Miki, M.; Fumiyuki, O., Platinum(0)-Catalyzed Diboration of Alkynes with Tetrakis(alkoxo)diborons: An Efficient and Convenient Approach to cis-Bis(boryl)alkenes. Organometallics, 1996; Vol. 15, pp 713-720.

13. Brown, S. D.; Armstrong, R. W., Parallel Synthesis of Tamoxifen and Derivatives on Solid Support via Resin Capture. *The Journal of organic chemistry* **1997,** *62* (21), 7076-7077.

14. (a) Marsaud, V.; Gougelet, A.; Maillard, S.; Renoir, J. M., Various phosphorylation pathways, depending on agonist and antagonist binding to endogenous estrogen receptor alpha (ERalpha), differentially affect ERalpha extractability, proteasome-mediated stability, and transcriptional activity in human breast cancer cells. *Molecular endocrinology* **2003,** *17* (10), 2013-2027; (b) Wittmann, B. M.; Sherk, A.; McDonnell, D. P., Definition of functionally important mechanistic differences among selective estrogen receptor down-regulators. *Cancer research* **2007,** *67* (19), 9549-9560.

15. (a) Detre, S.; Riddler, S.; Salter, J.; A'Hern, R.; Dowsett, M.; Johnston, S. R., Comparison of the selective estrogen receptor modulator arzoxifene (LY353381) with tamoxifen on tumor growth and biomarker expression in an MCF-7 human breast cancer xenograft model. *Cancer research* **2003,** *63* (19), 6516-6522; (b) Deshmane, V.; Krishnamurthy, S.; Melemed, A. S.; Peterson, P.; Buzdar, A. U., Phase III double-blind trial of arzoxifene compared with tamoxifen for locally advanced or metastatic breast cancer. *Journal of clinical oncology : official journal of the American Society of Clinical Oncology* **2007,** *25* (31), 4967-4973.

16. Greenberger, L. M.; Annable, T.; Collins, K. I.; Komm, B. S.; Lyttle, C. R.; Miller, C. P.; Satyaswaroop, P. G.; Zhang, Y.; Frost, P., A new antiestrogen, 2-(4-hydroxy-phenyl)-3-methyl-1-[4-(2-piperidin-1-yl-ethoxy)-benzyl]-1H-indol-5-o l hydrochloride (ERA-923), inhibits the growth of tamoxifen-sensitive and -resistant tumors and is devoid of uterotropic effects in mice and rats. *Clinical cancer research : an official journal of the American Association for Cancer Research* **2001,** *7* (10), 3166-3177.

17. Poupaert, J.; Carato, P.; Colacino, E.; Yous, S., 2(3H)-benzoxazolone and bioisosters as "privileged scaffold" in the design of pharmacological probes. *Current medicinal chemistry* **2005,** *12* (7), 877-885.

18. Leeson, P. D.; Springthorpe, B., The influence of drug-like concepts on decision-making in medicinal chemistry. *Nature reviews. Drug discovery* **2007,** *6* (11), 881-890.

19. Ashby, J.; Odum, J.; Foster, J. R., Activity of raloxifene in immature and ovariectomized rat uterotrophic assays. *Regulatory toxicology and pharmacology : RTP* **1997,** *25* (3), 226-231.

20. Stepan, A. F.; Walker, D. P.; Bauman, J.; Price, D. A.; Baillie, T. A.; Kalgutkar, A. S.; Aleo, M. D., Structural alert/reactive metabolite concept as applied in medicinal chemistry to mitigate the risk of idiosyncratic drug toxicity: a perspective based on the critical examination of trends in the top 200 drugs marketed in the United States. *Chemical research in toxicology* **2011,** *24* (9), 1345-1410.

21. Rosati, R. L.; Da Silva Jardine, P.; Cameron, K. O.; Thompson, D. D.; Ke, H. Z.; Toler, S. M.; Brown, T. A.; Pan, L. C.; Ebbinghaus, C. F.; Reinhold, A. R.; Elliott, N. C.; Newhouse, B. N.; Tjoa, C. M.; Sweetnam, P. M.; Cole, M. J.; Arriola, M. W.; Gauthier, J. W.; Crawford, D. T.; Nickerson, D. F.; Pirie, C. M.; Qi, H.; Simmons, H. A.; Tkalcevic, G. T., Discovery and preclinical pharmacology of a novel, potent, nonsteroidal estrogen receptor agonist/antagonist,

CP-336156, a diaryltetrahydronaphthalene. *Journal of medicinal chemistry* **1998,** *41* (16), 2928-2931.

22. Grese, T. A.; Cho, S.; Finley, D. R.; Godfrey, A. G.; Jones, C. D.; Lugar, C. W., 3rd; Martin, M. J.; Matsumoto, K.; Pennington, L. D.; Winter, M. A.; Adrian, M. D.; Cole, H. W.; Magee, D. E.; Phillips, D. L.; Rowley, E. R.; Short, L. L.; Glasebrook, A. L.; Bryant, H. U., Structure-activity relationships of selective estrogen receptor modulators: modifications to the 2-arylbenzothiophene core of raloxifene. *Journal of medicinal chemistry* **1997,** *40* (2), 146-167.

23. (a) Benet, L. Z.; Spahn-Langguth, H.; Iwakawa, S.; Volland, C.; Mizuma, T.; Mayer, S.; Mutschler, E.; Lin, E. T., Predictability of the covalent binding of acidic drugs in man. *Life sciences* **1993,** *53* (8), PL141-146; (b) Baba, A.; Yoshioka, T., Structure-activity relationships for degradation reaction of 1-beta-o-acyl glucuronides: kinetic description and prediction of intrinsic electrophilic reactivity under physiological conditions. *Chemical research in toxicology* **2009,** *22* (1), 158-172.

24. Kim, K. A.; Park, P. W.; Kim, K. R.; Park, J. Y., Effect of multiple doses of montelukast on the pharmacokinetics of rosiglitazone, a CYP2C8 substrate, in humans. *British journal of clinical pharmacology* **2007,** *63* (3), 339-345.

25. Lee, J. S.; Ettinger, B.; Stanczyk, F. Z.; Vittinghoff, E.; Hanes, V.; Cauley, J. A.; Chandler, W.; Settlage, J.; Beattie, M. S.; Folkerd, E.; Dowsett, M.; Grady, D.; Cummings, S. R., Comparison of methods to measure low serum estradiol levels in postmenopausal women. *J Clin Endocrinol Metab* **2006,** *91* (10), 3791-3797.

26. Fulvestrant Package insert: http://www1.astrazeneca-us.com/pi/faslodex.pdf.

27. Tamoxifen itself (60 mg/Kg po QD, 28 days) was found to have agonist activity in this tamoxifen-resistant xenograft, increasing tumor volume above vehicle: Tumor volume fold over start = 4.4 (versus vehicle tumor volume fold over start of 2.6), n=2 studies.

TABLE OF CONTENTS GRAPHIC

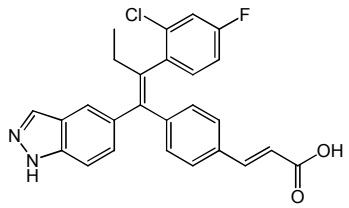

11l (GDC-0810 or ARN-810)
ER-α degradation IC_{50} = 0.7 nM
ER-α degradation Efficacy = 91%

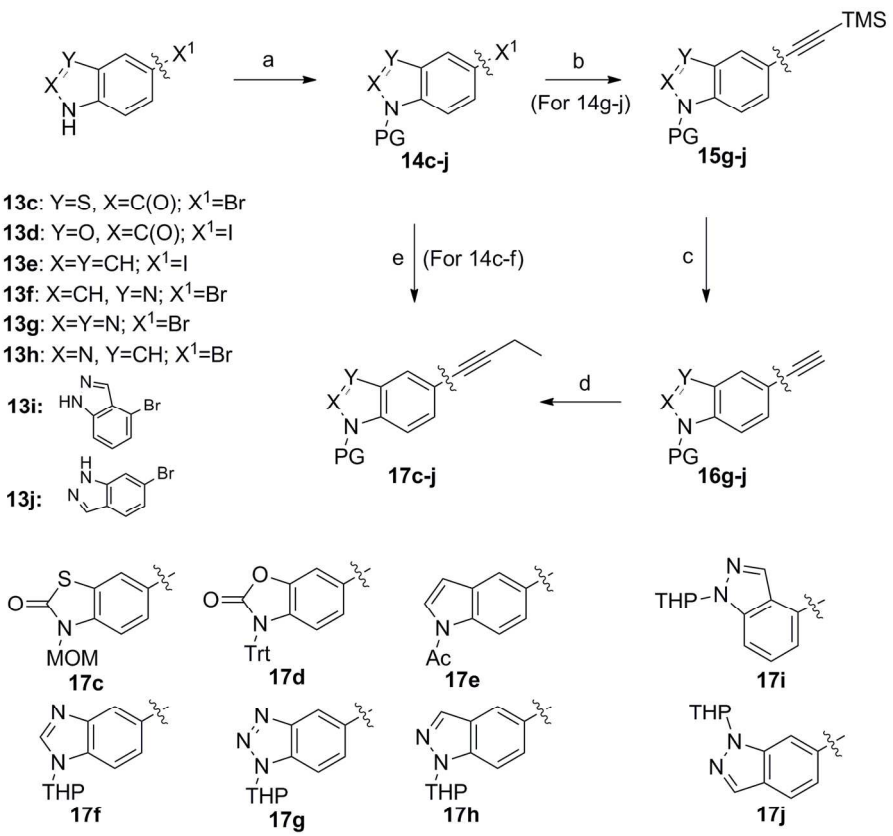

[a]Reagents and conditions: (a) For **13c**: MOM; MOM-Cl, K_2CO_3, DMF, 96%; **13d**: Tr-Cl, TEA, DCM, 83%; **13e**: Ac_2O, TEA, DMAP, DCE, 97%; **13f-j**: DHP, PPTS, DCM, 56-89%; (b) cat. $Pd(Ph_3P)_2Cl_2$,CuI, trimethylsilylacetylene, THF-TEA (5:1), 80 °C, 97-100%; (c) K_2CO_3, MeOH, rt, 49-98%; (d) n-BuLi, Et-I, THF/TMEDA (9:1), -78 °C-40 °C, 52-58%; (e) cat. $Pd(OAc)_2$, dppf, CuI, Cs_2CO_3, but-1-yn-1-yltrimethylsilane, DMA 80 °C, 47-93%.

164x163mm (300 x 300 DPI)

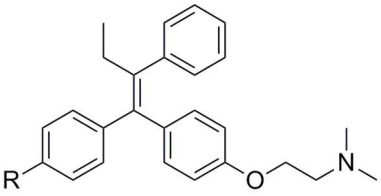

1: R = H: Tamoxifen
2: R = OH: 4-Hydroxytamoxifen

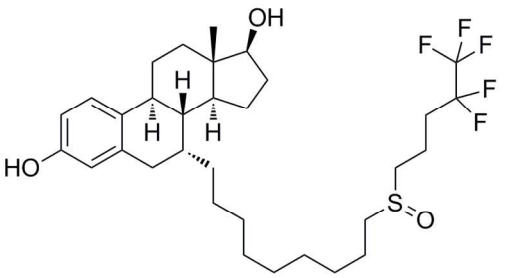

3: Fulvestrant

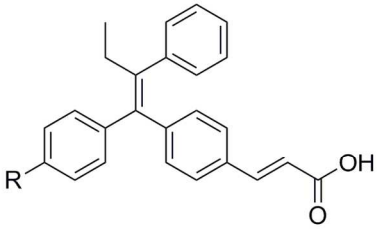

4: R = H: GW-5638
5: R = OH: GW-7604

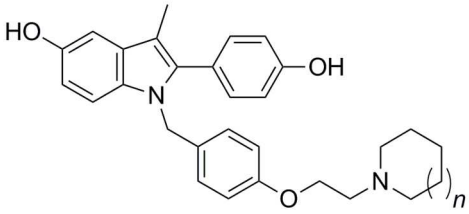

6: Pipendoxifene (*n* = 1)
7: Bazedoxifene (*n* = 2)

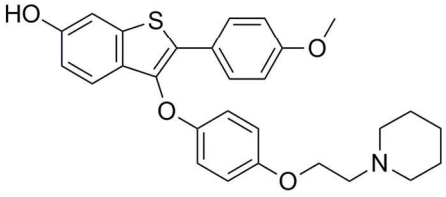

8: Arzoxifene

144x135mm (300 x 300 DPI)

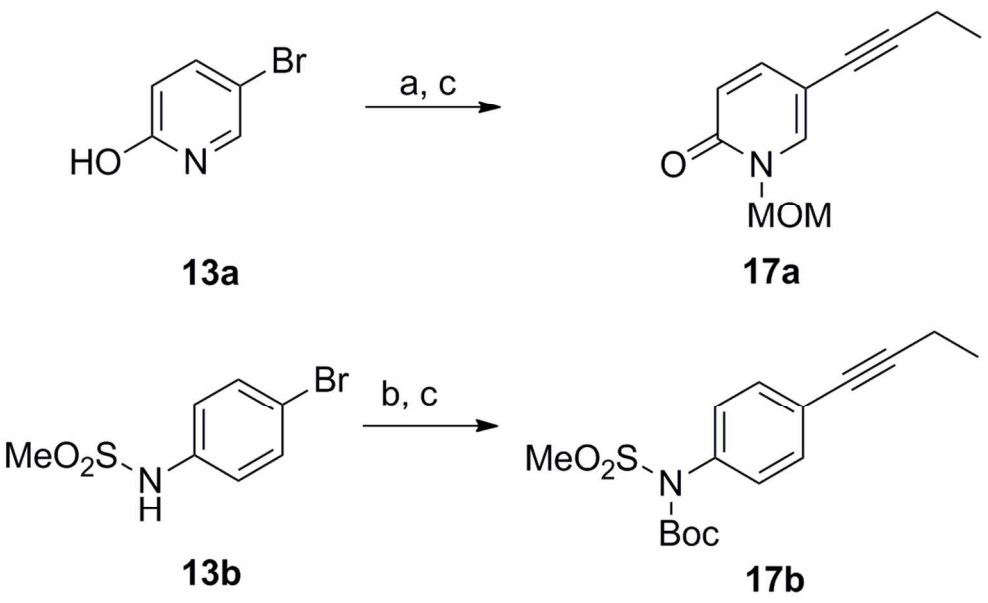

[a]Reagents and conditions: (a) MOM-Cl, K_2CO_3, DMF 40%; (b) Boc_2O, DMAP, DCM, 83%; (c) $Pd(OAc)_2$, dppf, CuI, Cs_2CO_3, but-1-yn-1-yltrimethylsilane 72-77%

100x80mm (300 x 300 DPI)

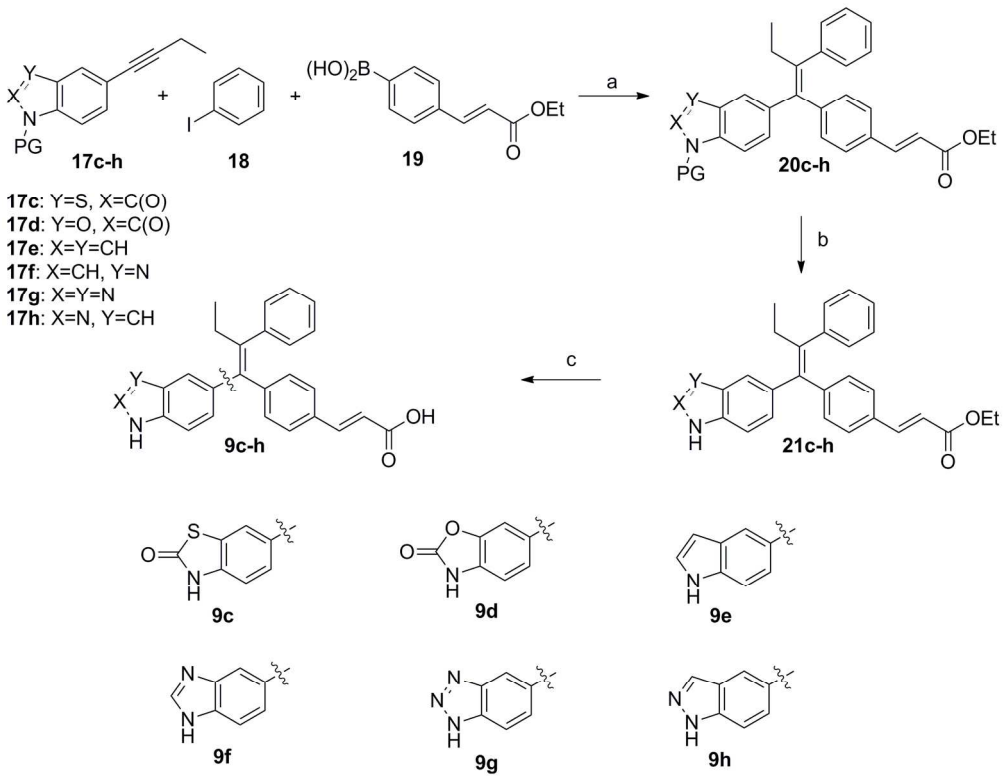

[a]Reagents and conditions: (a) cat. $Pd(PhCN)_2Cl_2$, K_2CO_3 , DMF/H_2O, 13-82%; (b) HCl, EtOH, 90-100%; (c) LiOH, THF-EtOH, 45-60%

177x154mm (300 x 300 DPI)

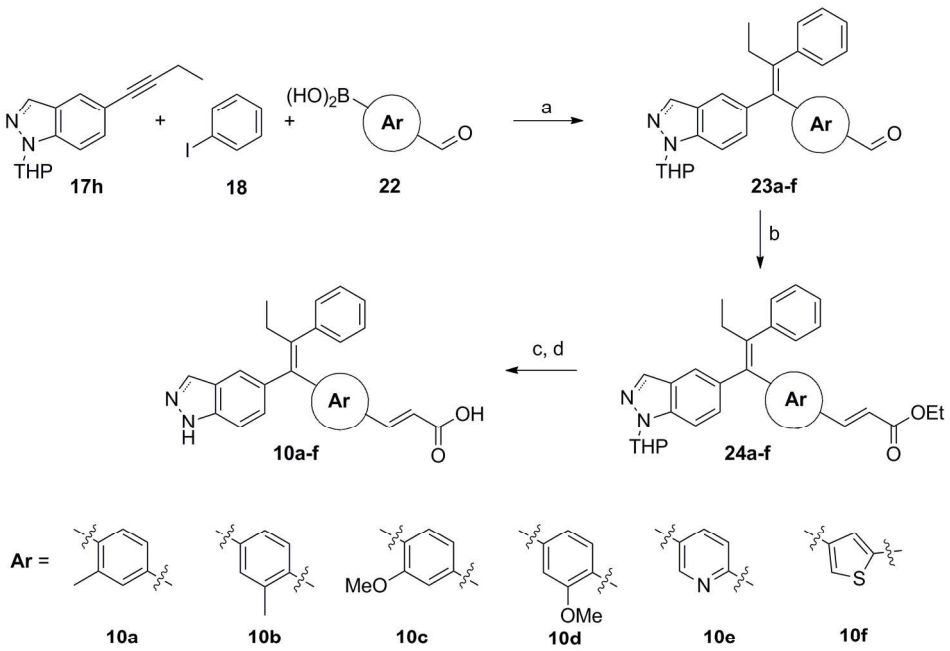

[a]Reagents and conditions: (a) cat. $Pd(PhCN)_2Cl_2$, K_2CO_3 , DMF/H_2O, 30-68%; (b) Triethylphosphonoacetate, LiCl, DBU, MeCN, 75-100%; (c) HCl, EtOH, 90-100%; (d) LiOH, THF-Et_2O, 54-60%

179x132mm (300 x 300 DPI)

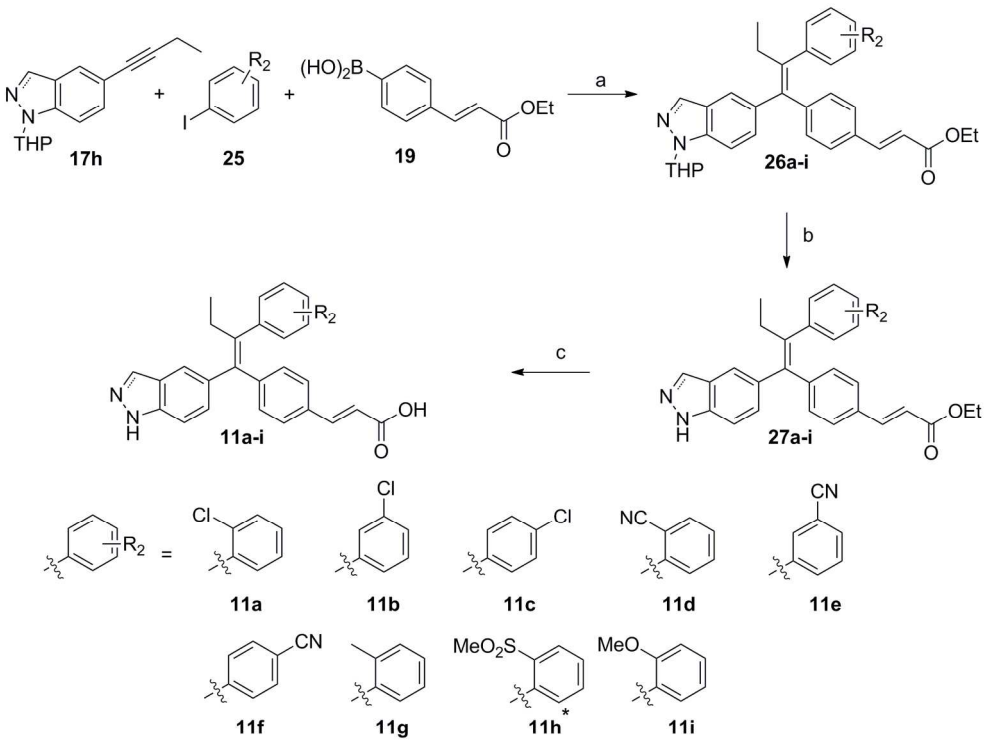

[a]Reagents and conditions: (a) cat. $Pd(PhCN)_2Cl_2$, K_2CO_3, DMF/H_2O, 8-62%; (b) HCl, EtOH, 95-100%; (c) LiOH, THF-EtOH, 11-77%; *2-iodothioanisole (**25**) was used in step (a) followed by oxone oxidation to give **26h**.

180x149mm (300 x 300 DPI)

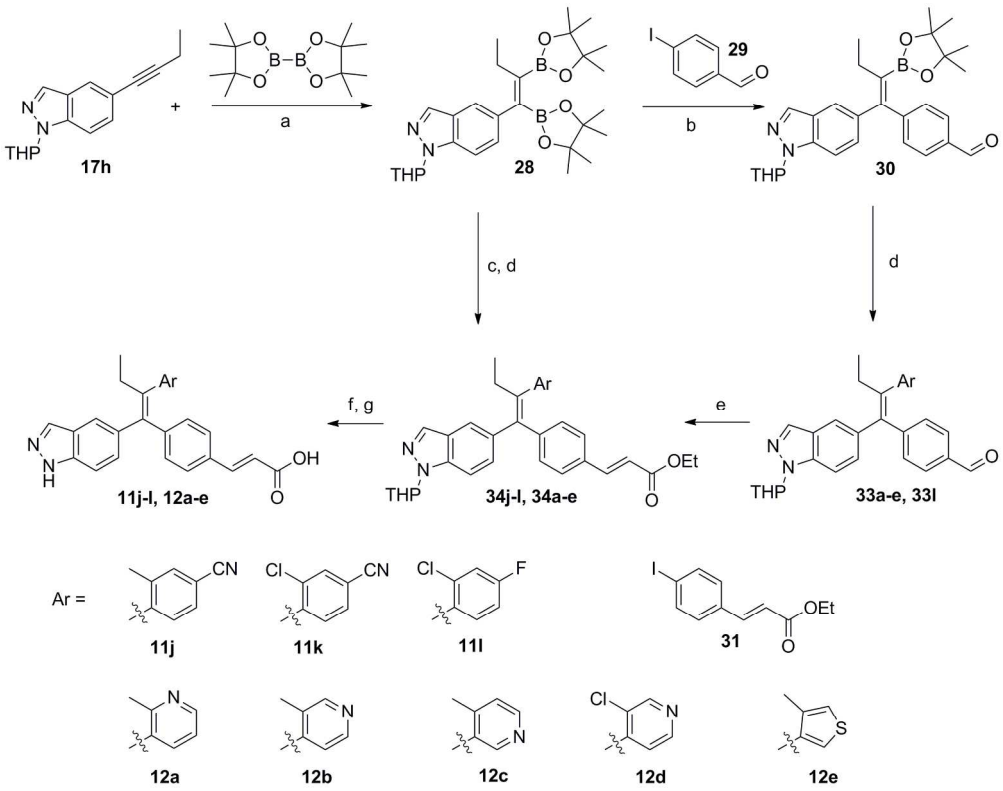

[a]Reagents and conditions: (a) cat. $Pt(PPh_3)_4$, bis(pinacolato)diboron, 2-MeTHF, 80 °C; (b) **29**, cat. $PdCl_2(PPh_3)_2$, Cs_2CO_3, 2-MeTHF, 0 °C-rt; (c) **31,** cat. $PdCl_2(PPh_3)_2$, Cs_2CO_3, 2-MeTHF, 0 °C-rt; (d) Ar-X **(32)**, cat. $PdCl_2(PPh_3)_2$, KOH (or K_2CO_3 in 1:1 2-MeTHF/DMSO), 2-MeTHF, reflux 21-99% (3 steps); (e) Triethyl-phosphonoacetate, LiCl, DBU, MeCN, rt, 56-96%; (f) HCl, EtOH; (g) LiOH, THF-EtOH, 26-93% (2 steps)

196x179mm (300 x 300 DPI)